

Nano-Iron Oxide (Fe_3O_4) Mitigates the Effects of Microplastics on a Ryegrass Soil–Microbe–Plant System

Dong Liu, Shahid Iqbal, Heng Gui,* Jianchu Xu, Shaoshan An, and Baoshan Xing



Cite This: <https://doi.org/10.1021/acsnano.3c05809>



Read Online

ACCESS |



Metrics & More



Article Recommendations

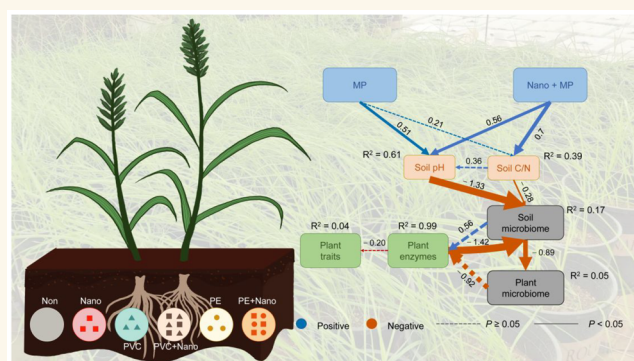


Supporting Information

ABSTRACT: To understand microplastic–nanomaterial interactions in agricultural systems, a randomized block 90-day pot experiment was set up to cultivate ryegrass seedlings in a typical red sandy soil amended with compost (1:9 ratio). Polyvinyl chloride (PVC) and polyethylene (PE) microplastic (MP) contaminants were added into pot soils at 0.1 and 10%, whereas nano- Fe_3O_4 (as nanoenabled agrochemicals) was added at 0.1% and 0.5% in comparison with chemical-free controls. The combination of nano- Fe_3O_4 and MPs significantly increased the soil pH (+3% to +17%) but decreased the total nitrogen content (−9% to −30%; $P < 0.05$). The treatment group with both nano- Fe_3O_4 and PE had the highest total soil C (29 g kg^{-1} vs 20 g kg^{-1} in control) and C/N ratio (13 vs 8 in control).

Increased rhizosphere nano- Fe_3O_4 concentrations promoted ryegrass growth (+42% dry weight) by enhancing the chlorophyll (+20%) and carotenoid (+15%) activities. Plant leaf and root peroxidase enzyme activity was more significantly affected by nano- Fe_3O_4 with PVC (+15%) than with PE (+6%). Nano- Fe_3O_4 significantly changed the ryegrass bacterial community structure from belowground (the rhizosphere and root endosphere) to aboveground (the phylloplane). Under MP contamination, the addition of nano- Fe_3O_4 increased bacterial diversity (+0.35%) and abundance (+30%) in the phylloplane and further intensified the connectivity of ryegrass aboveground bacterial networks (positive association increased 17%). The structural equation model showed that the change in the plant microbiome was associated with the rhizosphere microbiome. Overall, these findings imply the positive influences of nano- Fe_3O_4 on the soil–microbe–plant system and establish a method to alleviate the harmful effects of MP accumulation in soils.

KEYWORDS: grass, microbiome, microplastics, nanoparticles, soils, ryegrass



INTRODUCTION

The numerous applications of plastics, mainly due to their flexible surfaces and lightweight nature, have greatly boosted plastic production since 1950 to the current manufacture of more than 12.5 million tons annually.^{1,2} The prevalent use of plastics is projected to generate around 12 billion tons of plastic debris by 2050, and this is likely to lead to severe environmental issues.^{3,4} Microplastic (MP) particles of synthetic organic polymers with sizes <5 mm have emerged as dangerous pollutants since 1980, and much attention has been paid to the MPs and their relevant health issues.^{5,6} MPs with different shapes and morphologies such as pellets, fibers, foams, and films have been reported to spread in the atmosphere, terrestrial, aquatic, and soil environments, posing a threat to living beings.^{7,8} Therefore, MP contamination has been intensifying/escalating rapidly, gaining a lot of research attention and generating the need to understand the impact of

MPs on terrestrial environments, especially agriculture. Although the use of plastic in agriculture initially promoted food security worldwide, today it is well-known that it has left a pollution legacy, as MPs threaten food production systems.⁹

The loading of polyethylene (PE) in the soil is extremely common due to the extensive use of PE mulch in agriculture.¹⁰ PE raw material is preferably used to produce mulch that is difficult to degrade, causing PE accumulation.^{11,12} A growing body of evidence has become available that shows that PE MPs

Received: June 27, 2023

Revised: December 5, 2023

Accepted: December 8, 2023



ACS Publications

© XXXX American Chemical Society

A

<https://doi.org/10.1021/acsnano.3c05809>
ACS Nano XXXX, XXX, XXX–XXX

Table 1. Physicochemical Properties of Ryegrass Rhizosphere Soils with Different Microplastic (PVC and PE) and/or Nano-Fe₃O₄ Additions^a

treatment	pH	total C (g kg ⁻¹)	total N (g kg ⁻¹)	C:N ratio	organic matter (g kg ⁻¹)	Fe ₂ O ₃ (mg kg ⁻¹)
control	6.53 ± 0.02d	19.97 ± 0.65bc	2.45 ± 0.21a	8.20 ± 0.83e	45.6 ± 3.7c	208 ± 2.4a
nano-Fe ₃ O ₄	6.74 ± 0.08c	20.20 ± 0.09b	2.06 ± 0.03bc	9.79 ± 0.17d	52.8 ± 10.7b	207 ± 4.2a
PVC	7.10 ± 0.05b	18.99 ± 0.58c	2.03 ± 0.05c	9.37 ± 0.31d	34.2 ± 2.7d	147 ± 3.8c
PVC + nano-Fe ₃ O ₄	7.06 ± 0.09b	19.84 ± 0.4bc	1.83 ± 0.04d	10.86 ± 0.34c	41.6 ± 7.6c	117 ± 10.1d
PE	7.16 ± 0.07b	20.53 ± 0.28b	1.70 ± 0.03d	12.06 ± 0.10b	58.9 ± 4.6ab	195 ± 4.0b
PE + nano-Fe ₃ O ₄	7.67 ± 0.12a	29.09 ± 0.92a	2.23 ± 0.08b	13.06 ± 0.10a	74.1 ± 3.2a	184 ± 1.7b

^aNote: the significance tests among chemical treatments are based on the least significant difference (LSD) test ($n = 4$, $P < 0.05$).

may alter the physical and chemical conditions of soil.¹³ In particular, several soil properties that are indicators of soil health, such as the pH, organic carbon, aggregation, aeration, organic matter (OM), water retention capacity, and nutrient (nitrogen (N) and phosphorus (P)) content and availability, are affected.^{13,14} PE MPs are also known to reduce seed germination by mechanically covering the pore of the seed.¹⁵ Moreover, the bioavailability of heavy metals such as Cd after soil contamination with PE reduces root growth and arbuscular mycorrhizal fungi symbiotic associations with plants.¹⁶ Soil biota are indicators of plant health and nutrient cycling and have a significant impact on soil ecosystem services. Recent studies have reported that PE MPs have the potential to alter microbial community composition and activities as well as the stability of microfood webs.¹⁷ Similarly, polyvinyl chloride (PVC) is one of the most commonly detected MPs in soil environments,¹⁸ and it has also substantial impacts on microbial abundance (such as Burkholderiaceae) and network stability, with wide implications for crop growth.^{19,20} Such impacts on soil microbes are due to either changes in soil properties or the release of impurities and chemical additives from plastics.²¹ Hence, the loading of PE and PVC MPs represents a major challenge for agroecosystems. Importantly, the concentration of these MPs in soil is most likely to have substantial impacts on the soil microbes and plant growth. For instance, the growth of romaine lettuce was found to decrease due to PE contamination at the rates of 0.005%, 0.025%, and 0.1% in the soil, although the impact of 0.1% was the greatest.²² A PE content of 1% in soil has been shown to negatively affect the above- and belowground compartments of wheat plants during both vegetative and reproductive growth.²³ In a recent experiment aimed at investigating the effects of MPs on plant performance, PE and PVC each at 0.2% and 1% concentrations appeared to affect the growth and reproduction biomass of native and invasive *Phytolacca* species.²⁴ In addition, a 0.1% content of high-density PE in soil can reduce the total biomass of perennial ryegrass through the alteration of soil stability components such as pH, organic matter, and water-stable aggregates.²⁵ Thus, MP contamination in grasslands represents an important concern within agricultural production systems.²⁶ However, information regarding the impacts of relatively higher doses of PE and PVC on the agroecosystem is scarce. In addition, extremely limited knowledge exists on how to protect the functioning of these ecosystems in cases whereby the PE and PVC concentrations in soil exceed the current stock.

To meet the global food production demand, using nanoparticles (NPs) that promote plant growth and help crops cope with environmental stress is becoming common in agriculture.²⁷ NPs can enhance plant disease resistance,²⁸ increase plant rhizosphere N-fixing bacteria,²⁹ and stimulate N

fixation and plant growth.³⁰ In terms of plant protection and fertilization, NP use has contributed tremendously to sustainable nanoenabled agricultural development.³¹ Among nanomaterials, the use of Fe₃O₄ is common because its positive influence has been reported in many crops.³² For example, the application of 500 mg L⁻¹ of Fe₃O₄ significantly promoted the fresh weight of barley leaves by 19% and roots by 88%³³ while the application of Fe₃O₄ (100 mg L⁻¹) was shown to promote maize plant growth.³⁴ The positive effects of Fe₃O₄ on soil microbes have also been reported, where for instance applying magnetic Fe₃O₄ NPs at the rates of 0.04%, 0.08%, and 0.26% could facilitate soil carbon (C) and N cycling by changing the bacterial community structure.³⁵ In particular, the abundance of N-fixation-related bacteria Bradyrhizobiaceae and iron-redox bacteria Sediminibacterium were noted to decline while the proliferation of *Duganella* and *Nocardioides* bacteria was observed. Additionally, nano-Fe₃O₄ application at the rate of 0.01% significantly increased the populations of carbon-cycling bacteria, *Nocardioides*, *Chitinophaga sancti*, *Pantoea*, and *Rhizobium* from 0.14 to 0.96, which constituted an average of 0.58% in relative abundance.³⁴ However, the use of Fe₃O₄ (0.2%) induced significant decline in the microbial biomass by up to 55%, 36% of mineral N content, and 125% reduction in N mineralization efficiency of sandy soil mainly due to the presence of labile Fe in the microbial biomass.³⁶ Thus, understanding the effects of Fe₃O₄ on both plants and microbes in soils and the relevant mechanisms is crucial for risk evaluation and sustainable agriculture practices. Practically, the amount of nanoscale Fe can be scaled up and produced in an economically feasible manner for that level of amendment on a per acre basis. Furthermore, Fe₃O₄ has the potential to magnetize MPs via surface adsorption³⁷ and this can facilitate the removal of MPs, especially from water bodies. Similarly, in soil environments, applied Fe₃O₄ can bind with PE and PVC and may reduce the negative effects of these MPs on plants and soil microbial life. However, empirical evidence of these beneficial effects associated with Fe₃O₄ is scarce. Consequently, studies evaluating interactions between MPs and Fe₃O₄ are important to achieving resilience against the adverse effects of MPs on the soil–plant system. This study evaluates the integrated responses of soil microbes and plant systems when exposed to both low and extremely high levels of MP contamination accompanied by nano-Fe₃O₄ addition using soil planted with ryegrass (*Lolium perenne*), a common perennial grass used in agriculture during the fallowing stage. The present study hypothesized that PVC and PE would adversely alter plant growth and physiological traits, as well as the soil physicochemical and biochemical properties, while the coapplication of nano-Fe₃O₄ and MPs would alleviate these effects. The findings will enhance the understanding of microplastic–nanomaterial interactions and provide important

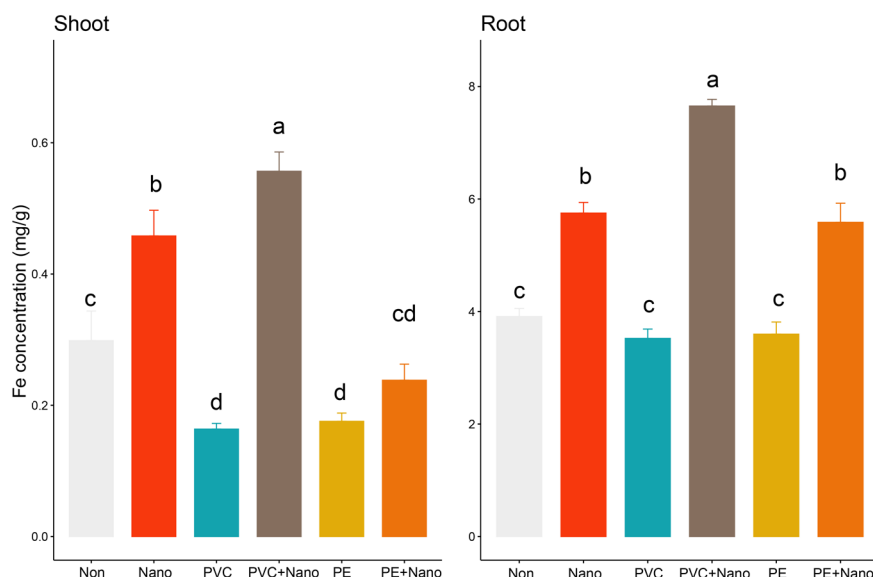


Figure 1. Effects of the addition of nano-Fe₃O₄ and microplastics (poly(vinyl chloride) (PVC) and polyethylene (PE)) on the Fe uptake of ryegrass shoots (a) and roots (b). Values are the means (SE) ($n = 12$); values followed by different letters are significantly different at $P < 0.05$ (analysis of variance (ANOVA), least significant difference (LSD) test).

information for the development of sustainable nanoenabled strategies to alleviate microplastic contamination in agricultural systems.

RESULTS AND DISCUSSION

Rhizosphere Soil Physicochemical Properties. Nano-Fe₃O₄ and MP addition, either individually or in combination, significantly increased the soil pH (+3% to +17%) but decreased (−9% to −30%; $P < 0.05$) the soil total N content (Table 1).

The combined application of PE and nano-Fe₃O₄ had the highest pH, total C, and C/N ratio, followed by the application of PE alone. However, the unamended control displayed the maximum total N. It was found that adding MPs (PE and PVC) and nano-Fe₃O₄ increased the ryegrass rhizosphere soil pH. The increased pH was in accordance with Yang's research,³⁸ regardless of plastic type, low-density PE or high-density PE. Such effects can be explained by the alteration of the soil acid–base equilibrium via changing the competitive sorption of hydrophobic organic compounds between MPs and soil OM.³⁹ Previous studies have shown that soil pH changes can affect soil nutrient mobility.⁴⁰ In this study, under the presence of nano-Fe₃O₄ and MPs, the increased soil pH might stimulate ryegrass N absorption, leading to a significant decrease (−9 to −30%) in the rhizosphere total N contents. However, the effects of nano-Fe₃O₄ on soil N (or soil C) varied with the MP type. This is because MPs made from various polymers with different properties have different effects on soil properties and biota.⁴¹ The structural aspect of MPs that affects chemical sorption is the glass transition temperature (T_g). Due to the pore-filling process of organic chemicals into PVC (glassy polymers, $T_g > T_{\text{ambient}}$), a nonlinear sorption isotherm was observed on PVC, which differed from the linear sorption isotherm for PE (rubbery polymers, $T_g < T_{\text{ambient}}$).³⁹ As a common soil component, Fe₂O₃ has a large proportion of colloid-based fractions. This was true in the red soil tested in the current study, which had the highest content of Fe₂O₃ (208 mg kg^{−1}; Table 1). However, under the presence of MPs

(either PE or PVC), the content of Fe₂O₃ decreased significantly ($P < 0.05$), which could be explained by the effects of MP-mediated pH and ionic composition changes on the sorption/desorption of soil OM on Fe compounds.⁴² As a key soil characteristic influencing Fe chemistry and behavior, OM influences the stability of Fe and redox processes associated with electron transfer processes.⁴³ When applying nano-Fe₃O₄ to MP-contaminated soils, the OM showed an increase but the content of Fe₂O₃ was decreased (Table 1). The increased soil OM (from 46 to 53 g kg^{−1}) under the addition of nano-Fe₃O₄ could be associated with the adsorption of fulvic acid (one of the humic substances) on the surfaces of Fe₃O₄ NPs through chemical reactions.⁴⁴ Nanomaterials are known to have a wide range of potential applications in agriculture, including providing efficient nutrient delivery, crop protection strategies, and responsive phytohormones.^{45,46} In comparison to chelated Fe, the nano-Fe was the most efficient source of Fe and it can enhance Fe solubility and its subsequent uptake by the plant (either by roots or leaves) due to its smaller particle size and larger surface area.⁴⁷ For example, foliar application of nano-Fe can lead to greater growth than conventional Fe chelates.⁴⁸ Research works have indicated the positive and enhancing effects of nano-Fe fertilization on plant growth and yield.³⁰

Plant Fe Uptake, Plant Growth, and Physiological Traits. The uptake of Fe was over 15 times higher in the ryegrass shoots (~5 mg g^{−1}) than in roots (~0.3 mg g^{−1}), indicating that Fe was mainly transferred and stabilized in plant shoots. Compared to the control, MPs decreased the Fe content in shoots (−76%, $P < 0.05$) and roots (−8%, $P < 0.05$) (Figure 1), showing that MPs could decrease the available Fe concentration in the rhizosphere and Fe uptake in the aboveground parts of plants. This should be associated with the negative effects of MPs in belowground soil environments such as decreased pH, reduced soil stability, and significantly decreased microaggregates (<63 μm),²⁵ and the variations in soil physicochemical characteristics and structure could further impair plant Fe acquisition systems and the major components

Table 2. Effects of the Nano-Fe₃O₄ and Microplastic (Polyvinyl Chloride (PVC) and Polyethylene (PE)) Additions on the Growth and Physiological Traits of Ryegrass

treatment (w/w soil)	root length (cm)	dry weight (g)	Fv/Fm	chlorophyll A (mg g ⁻¹)	chlorophyll B (mg g ⁻¹)	carotenoids (mg g ⁻¹)
control	18.62 ± 3.47a	0.17 ± 0.13a	0.79 ± 0.06a	1.4 ± 0.24abc	0.4 ± 0.07a	0.32 ± 0.05ab
0.01% Fe ₃ O ₄	20.84 ± 3.00a	0.26 ± 0.10a	0.87 ± 0.08a	1.47 ± 0.19abc	0.39 ± 0.06a	0.34 ± 0.04ab
0.05% Fe ₃ O ₄	25.3 ± 7.27a	0.37 ± 0.13a	0.74 ± 0.02a	1.73 ± 0.34ab	0.48 ± 0.12a	0.39 ± 0.06ab
1% PVC	22.42 ± 6.2a	0.32 ± 0.13a	0.78 ± 0.08a	1.88 ± 0.31a	0.55 ± 0.12a	0.47 ± 0.13a
1% PVC + 0.01% Fe ₃ O ₄	23.26 ± 7.9a	0.22 ± 0.10a	0.75 ± 0.07a	1.62 ± 0.38abc	0.50 ± 0.14a	0.39 ± 0.09ab
1% PVC + 0.05% Fe ₃ O ₄	26.5 ± 13.9a	0.26 ± 0.16a	0.80 ± 0.06a	1.49 ± 0.04abc	0.42 ± 0.02a	0.35 ± 0.01ab
10% PVC	28.0 ± 5.38a	0.28 ± 0.11a	0.83 ± 0.09a	1.31 ± 0.30bc	0.46 ± 0.18a	0.30 ± 0.07b
10% PVC + 0.01% Fe ₃ O ₄	28.8 ± 4.14a	0.41 ± 0.22a	0.77 ± 0.09a	1.44 ± 0.11abc	0.41 ± 0.07a	0.33 ± 0.02ab
10% PVC + 0.05% Fe ₃ O ₄	27.1 ± 9.22a	0.41 ± 0.04a	0.73 ± 0.01a	1.48 ± 0.18abc	0.45 ± 0.06a	0.34 ± 0.04ab
1% PE	23.75 ± 1.19a	0.30 ± 0.09a	0.77 ± 0.10a	1.42 ± 0.45abc	0.41 ± 0.09a	0.32 ± 0.12ab
1% PE + 0.01% Fe ₃ O ₄	31.20 ± 5a	0.35 ± 0.09a	0.78 ± 0.06a	1.42 ± 0.11abc	0.41 ± 0.02a	0.33 ± 0.02ab
1% PE + 0.05% Fe ₃ O ₄	22.90 ± 4.47a	0.32 ± 0.11a	0.77 ± 0.06a	1.27 ± 0.16bc	0.37 ± 0.03a	0.30 ± 0.03b
10% PE	24.10 ± 5.6a	0.34 ± 0.16a	0.74 ± 0.01a	1.15 ± 0.22c	0.35 ± 0.05a	0.27 ± 0.06b
10% PE + 0.01% Fe ₃ O ₄	23.50 ± 2.78a	0.25 ± 0.05a	0.79 ± 0.10a	1.34 ± 0.42abc	0.39 ± 0.09a	0.31 ± 0.1b
10% PE + 0.05% Fe ₃ O ₄	31.40 ± 10.9a	0.40 ± 0.13a	0.85 ± 0.10a	1.65 ± 0.29abc	0.48 ± 0.11a	0.39 ± 0.06ab

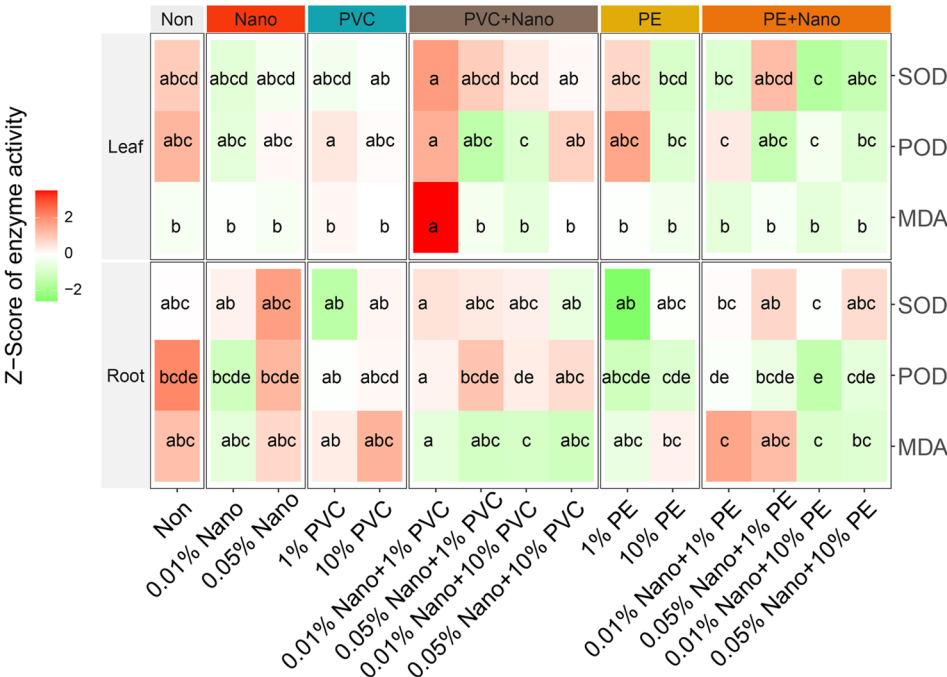


Figure 2. Effects of the addition of nano-Fe₃O₄ and microplastics (poly(vinyl chloride) (PVC) and polyethylene (PE)) on the malondialdehyde (MDA), superoxide dismutase (SOD), and peroxidase (POD).

that regulate Fe uptake systems.⁴⁹ However, when nano-Fe₃O₄ was applied to MP-contaminated soils, the Fe uptake was significantly increased in the roots (+116% in the PVC treatment; +30% in the PE treatment; Figure 1). The observed result reflected the positive effect of nano-Fe₃O₄ in mitigating the negative effects of MPs on plant Fe uptake and subsequent growth. Such positive effects can be attributed to (i) the strong adherence of nano-Fe₃O₄ on the MPs surface which weakens MP's ecotoxicology on plants^{37,50} and (ii) the positive effects of nano-Fe₃O₄ in facilitating plant rhizosphere nutrient cycling³⁵ and increasing plant growth promoting microbes.⁵¹

Photosynthesis is a key physiological process that is affected by different plant stresses. The addition of nano-Fe₃O₄ and/or MPs exerted weak stresses on ryegrass, as shown by a slight decrease (−3% on average) of the Fv/Fm (a chlorophyll fluorescence parameter reflecting the maximum quantum efficiency of photosystem II (PSII) photochemistry) in the majority of treatments (10 of 14). There were strong increases in ryegrass root length (+21.6%; 20.8–25.3 cm) and dry weight (+42.3%; 0.26–0.37 g) when the concentration of plant rhizosphere nano-Fe₃O₄ increased from 0.01 to 0.05%. This can be explained by (i) the effect of nano-Fe₃O₄ on plant growth promotion via improved soil N-

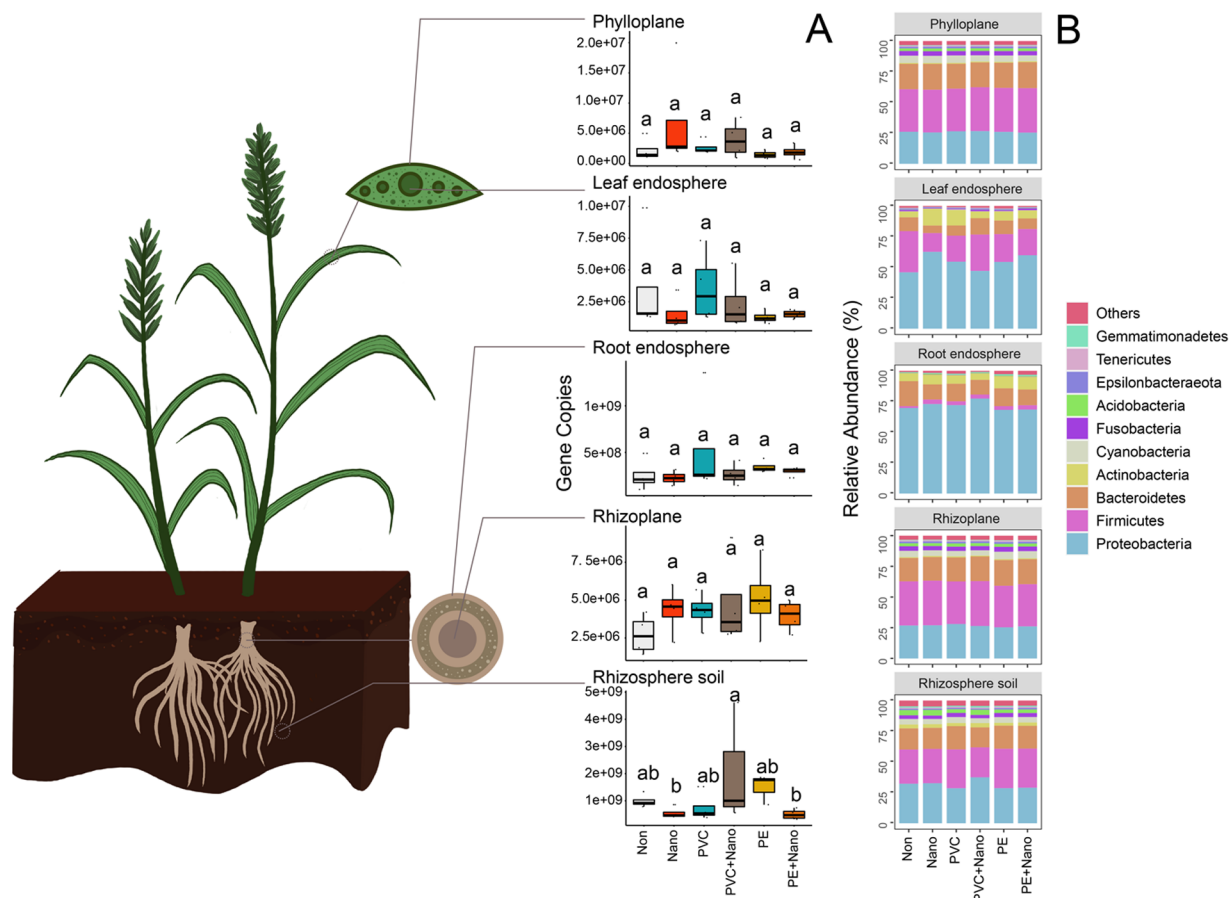


Figure 3. Effects of the nano-Fe₃O₄ and microplastics (polyvinyl chloride (PVC) and polyethylene (PE)) on the ryegrass bacterial gene copy numbers (A) and the relative abundance of endophytic bacterial phyla (B) in the above- and belowground compartments. Relative abundances of uncultured and unclassified/unidentified taxa are grouped as “Others”. Values are the mean values ($n = 4$). Different letters indicate significant differences at $P < 0.05$ based on the least significant difference (LSD) test.

use efficiency,³² (ii) the nanozyme-like attribute of nano-Fe₃O₄, which reduced plant hydrogen peroxide content under an increased nano-Fe₃O₄ dose,³³ and (iii) the uptake and translocation of nano-Fe₃O₄ by roots and leaves, which enhanced plant growth without phytotoxic effects.³³ Furthermore, nano-Fe₃O₄ enhanced the absorption and transfer of light energy and chlorophyll in the aboveground grass, as indicated by the increases in chlorophyll A (+18%; from 1.47 to 1.73 mg/g), chlorophyll B (+23%; from 0.39 to 0.48 mg/g), and carotenoids (+15%; from 0.34 to 0.39 mg/g), although the increases were not statistically significant (Table 2). Moreover, these physiological indicators reflected the strengthening of plant photosynthesis and the carbon–oxygen cycle, which can be explained by the function of nano-Fe₃O₄ in increasing the abundance of plant rhizosphere bacterial taxa associated with growth promotion and carbon cycling.⁵¹ The effects of nano-Fe₃O₄ on the rhizosphere soil properties (pH and total C and N contents) of ryegrass were affected by the MP features, which could be associated with their varied effects (due to shape, size, and polymer type) on the soil pH, bulk density, and nutrient retention.^{21,52} Similarly, the results showed that the effect of nano-Fe₃O₄ on improving the aboveground biomass of ryegrass was also highly associated with the MP type and dose. For example, the treatments receiving high doses (10%) of PVC and nano-Fe₃O₄ had a stronger ryegrass growth-promoting effect than those receiving low doses (1%)

of PVC and nano-Fe₃O₄, and vice versa for the interaction between PE and nano-Fe₃O₄, suggesting the diverse effects of MPs (varying based on type and dose) and nano-Fe₃O₄ on ryegrass growth.

High doses of PVC can improve the soil's physical structure,²¹ which may increase the contact area between Fe particles and the plant rhizosphere by boosting the diffusion of nano-Fe₃O₄. The improved soil porosity could further accelerate soil enzyme activities involved in C, N, and P cycling, as shown by similar studies conducted on MP types such as polypropylene⁵³ and polyethylene.¹⁹ The regulation of soil porosity on enzymes may increase the uptake of nutrients by ryegrass and stimulate grass aboveground biomass and photosynthesis (as shown by increased chlorophyll A and carotenoid contents under high-dose PVC application). Furthermore, the results on plant enzymes also showed that ryegrass leaf and root peroxidase activities were significantly increased (+25%) with the addition of high-dose PVC and nano-Fe₃O₄.

Plant Enzymes. The enzyme activities varied significantly for nano-Fe₃O₄ and MP additions at different concentrations (Figure 2). The maximum increase in root superoxide dismutase (SOD), peroxidase (POD), and malondialdehyde (MDA) activities occurred with the addition of 0.01% nano-Fe₃O₄ and 1% PVC, and this was followed by PVC application alone. In the leaves, the SOD, POD, and MDA activities were

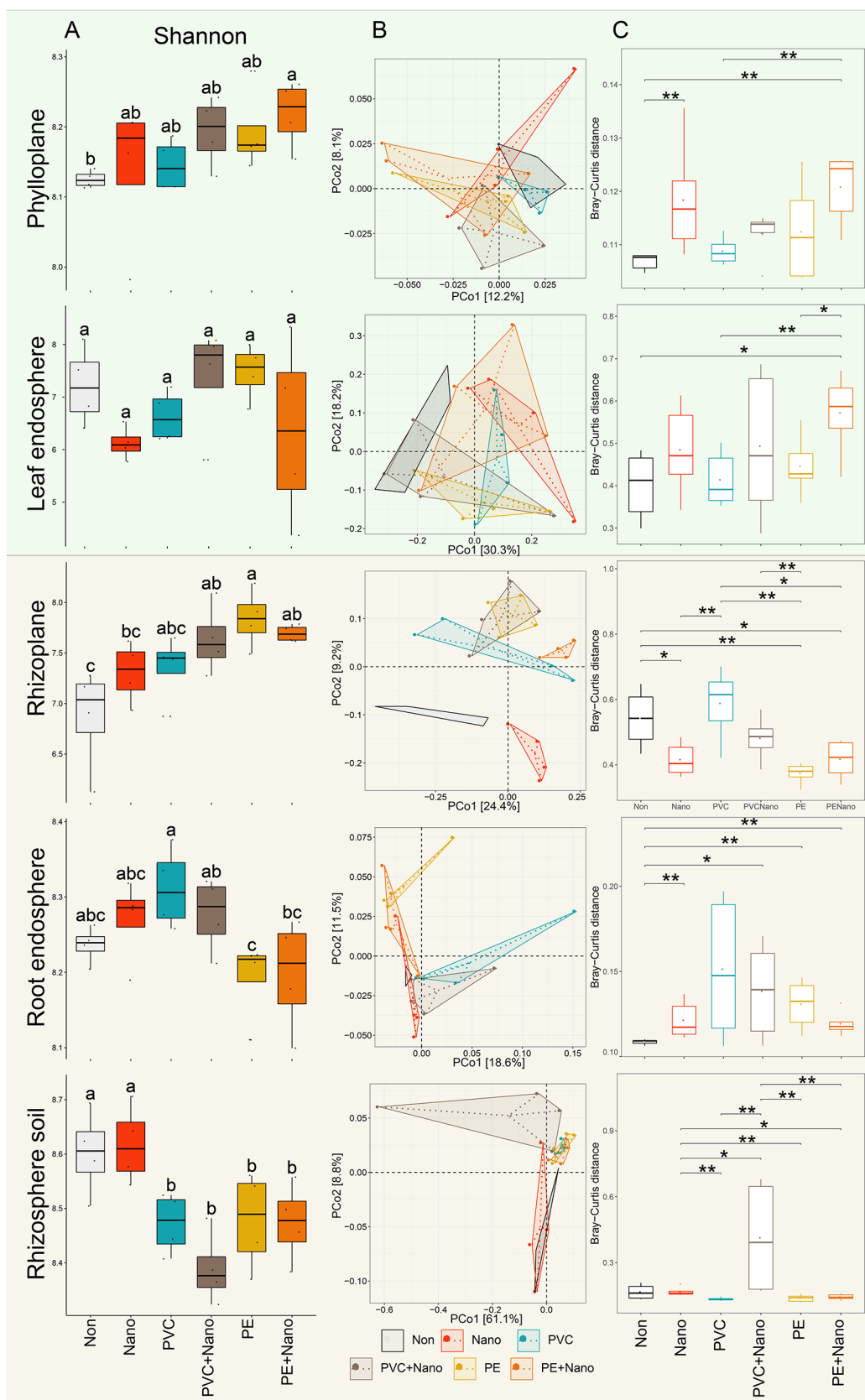


Figure 4. Effects of the nano- Fe_3O_4 and microplastics (polyvinyl chloride (PVC) and polyethylene (PE)) on ryegrass bacterial Shannon diversity (A), community in principal coordinate analysis (PCoA) (B), and community-based Bray–Curtis distance (C). Significant differences between treatments were detected using Tukey's multiple comparison test. * $P < 0.05$, ** $P < 0.01$.

highest with the addition of 0.01% nano-Fe₃O₄ and 1% PVC. Under the single nano-Fe₃O₄ treatments, ryegrass leaf and root enzyme activities, including SOD, POD, and MDA activities, increased with the increase in the nano-Fe₃O₄ concentration (0.01 vs 0.05%) (Figure 2). At the 1% (w/w) PVC condition, the increase of the nano-Fe₃O₄ concentration (from 0.01% to 0.05%) generally reduced the ryegrass leaf and root enzyme activities (Figure 2); however, at the high PVC concentration (10%), the accumulation of nano-Fe₃O₄ significantly increased ryegrass POD activity (+164% in leaves, +16.3% in roots) (Figure 2). These results indicated that the positive effect of nano-Fe₃O₄ application on ryegrass enzymes was diminished in soils containing 1% PVC. In contrast, in treatments receiving high doses of PVC (10%), the plant oxidative stress reaction (as revealed by POD activity) could be further increased.

In comparison, under the two levels of PE, the effect of nano-Fe₃O₄ accumulation increased the ryegrass SOD in both leaves and roots. However, for the other enzymes, the effect of nano-Fe₃O₄ was not significant with PE when compared to that with PVC treatments (Figure 2). In plants, both enzymatic and nonenzymatic antioxidants play an important role in neutralizing reactive oxygen species (ROS) to avoid possible oxidative damage.⁵⁴ Generally, excessive ROS levels can prompt cell membrane lipid peroxidation, which is indicated by an increased content of MDA, one of the final products of membrane lipid peroxidation. Therefore, MDA is used to indicate the extent of lipids resulting from oxidative stress.⁵⁵ In the present study, the accumulation of nano-Fe₃O₄ significantly increased plant antioxidant enzymes, which was in line with Cao et al.,³⁰ who demonstrated that nano-Fe₃O₄ activated the antioxidative system in plants. This could be associated with the uptake of NPs within plants because advanced nanotechnologies (i.e., inductively coupled plasma mass spectrometry and X-ray fluorescence imaging) have shown a clear size-dependent transport/uptake of NPs in plants.⁵⁶ Overall, the beneficial effects of nano-Fe₃O₄ on plants were size- and concentration-dependent; the smallest Fe yielded the highest growth promotion.³⁰ In the present study, the contents of the main root antioxidant enzymes, SOD and POD, with the addition of 0.05% nano-Fe₃O₄ were higher than those under 0.01% nano-Fe₃O₄. This suggested that 0.05% nano-Fe₃O₄ caused an oxidative stress reaction in the ryegrass roots. Furthermore, the MDA content in ryegrass leaves treated with 0.01% nano + 1% PVC was higher than that in other PVC + nano treatments. It is believed that this result is due to the root system absorbing 0.01% of the NPs and transporting them to the leaves.

Bacterial Community Composition and Structure.

The bacterial community size (absolute content) and composition across the compartments are given in Figure 3. In various compartments, namely, the leaf endosphere, phylloplane, root endosphere, and rhizoplane, the absolute bacterial abundance was not significantly affected by MP pollution either alone or in the presence of nano-Fe₃O₄ (Figure 3A). However, PVC with nano-Fe₃O₄ and PE alone increased the absolute bacterial abundance in the rhizosphere. In general, Proteobacteria was dominant in the leaf endosphere (contributing an average of 46% of the total bacterial abundance) and root endosphere (70%) after the addition of MPs either alone or in combination with nano-Fe₃O₄ (Figure 3B). However, the abundance of Bacteroidetes (~12 to 20%) and Firmicutes (13 to 33%) increased over 2-fold in the exterior ryegrass areas (the phylloplane and rhizoplane) and

the rhizosphere. Moreover, the effects of nano-Fe₃O₄ and MP addition (PVC and PE) were substantial at the bacterial family level, as detected using random forest analysis with bootstrapping. The numbers of significantly changed taxa were 9 in the phylloplane, 10 in the rhizoplane, 26 in the leaf endosphere, 33 in the root endosphere, and 238 in the rhizosphere (Figure S1 and Figure 3). The addition of nano-Fe₃O₄ significantly ($P < 0.05$) increased the abundances of Nocardioideaceae and Pseudonocardioideaceae in the leaf endosphere, Micavibrionaceae in the root endosphere, Microbacteriaceae and uncultured Planctomycetes in the rhizoplane, and Chthoniobacteriaceae, Acidobacteriaceae subgroup I, and Frankiaceae in rhizosphere soil (Figure S1 and Figure 3).

The Shannon diversity indices showed that the addition of nano-Fe₃O₄ alone had the highest bacterial diversity in the rhizosphere soil, followed by the control (no chemical addition) (Figure 4A). However, PVC and PE addition with or without nano-Fe₃O₄ increased the bacterial diversity in the rhizosphere to a lesser extent. In the root endosphere, the maximum increase in bacterial diversity occurred after sole PVC or PVC with nano-Fe₃O₄ addition.

For the rhizoplane, the bacterial diversity was at its maximum when soils were amended with PE. There were no significant differences in bacterial diversity among PE, PVC with nano-Fe₃O₄, and PE with nano-Fe₃O₄. However, in the phylloplane, nano-Fe₃O₄ addition with PE increased the ryegrass bacterial diversity.

The similarity of the bacterial community composition was analyzed using principal component analysis (PCoA) (Figure 4B). There was a clear separation of community composition between the control (no chemical addition) and other treatments for the rhizosphere, root endosphere, and rhizoplane. The community composition with nano-Fe₃O₄ addition formed clusters and was distinctly separated from the clusters of the control, sole MP addition, and the combination of different MPs with nano-Fe₃O₄. However, the bacterial community composition was not separated for all the treatments in the leaf endosphere and phylloplane.

Compared to the control, nano-Fe₃O₄ significantly ($P < 0.05$) changed the bacterial community composition from belowground (rhizoplane and root endosphere) to the aboveground phylloplane (Figure 4C). Moreover, PVC with nano-Fe₃O₄ significantly altered ($P < 0.05$) the bacterial community. In contrast, PE with nano-Fe₃O₄ changed the bacterial community composition in the leaf endosphere. When added individually, the three exogenous chemical additives increased the ryegrass endophytic bacterial community size, especially in the rhizoplane. This could be associated with enhanced soil macroporosity, which would facilitate plant root penetration,²¹ increasing the colonization and reproduction of rhizoplane bacteria. For the belowground compartment (the rhizoplane and root endosphere), the addition of nano-Fe₃O₄ with MPs (PVC and PE) decreased the root bacterial abundance. The results were in line with the single effects of MPs on soil bacterial diversity and richness,⁵⁷ implying that the commonly used nanomaterial may not neutralize the negative influence of MPs in soil.⁵⁸ However, when moving toward the aboveground, the endophytic bacterial abundance was increased in the phylloplane. Nano-Fe₃O₄ mediated the effects of MPs on ryegrass bacterial abundance, and such an effect was highly related to plant compartments. However, the implications of the compartment effect have not yet been elucidated. Under the PVC treatment, nano-Fe₃O₄ addition

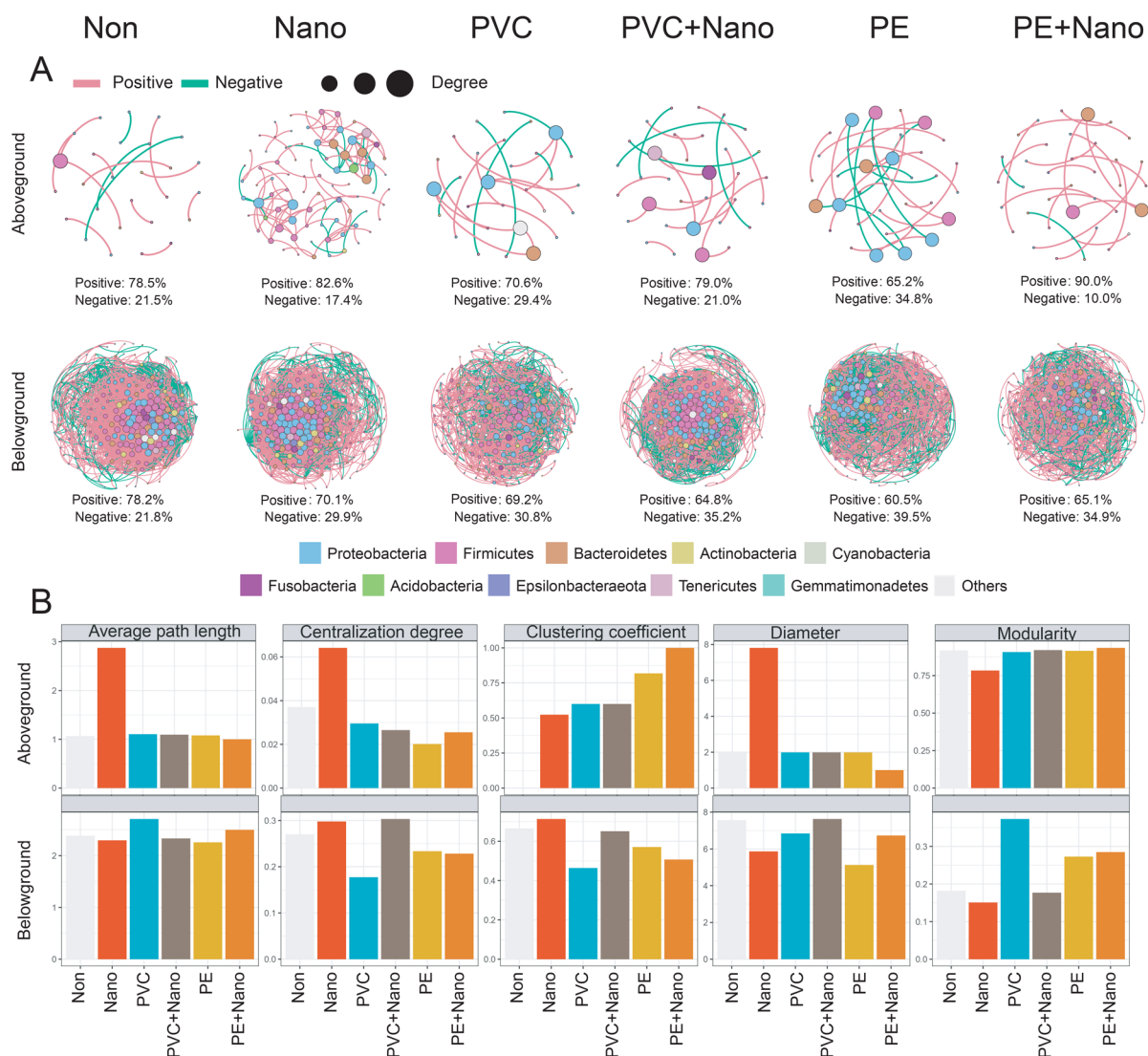


Figure 5. Effects of nano-Fe₃O₄ and microplastics (poly(vinyl chloride) (PVC) and polyethylene (PE)) on the above- and belowground ryegrass bacterial network interactions (A) and topological parameters (B). Nodes represent genera, and the colors of nodes indicate various major phyla. Solid lines represent relationships among bacterial genera, and a module is a cluster of highly interconnected bacterial genera. “Non” represents the control (no chemical addition treatment).

increased (~10%) the relative abundance of Proteobacteria in ryegrass roots. Many classes of Proteobacteria are eutrophic groups.⁵⁹ The abundance of Proteobacteria in the leaf and root endosphere of ryegrass may be closely related to their roles in promoting access to N and P, regulating the immune system, and enhancing plant resistance to pathogenic bacteria.^{60,61} There were significant increases of Bacteroidetes (~0.6 times in relative abundance) and Firmicutes (~1.5 times) in the compartments of ryegrass exposed to external environments such as the leaf surface, root surface, and rhizosphere. This selective accumulation of microbes could be related to their functions in environmental stress and disease resistance.⁶² Under different chemical treatments, nano-Fe₃O₄ addition increased the abundance of Proteobacteria, especially the Nocardioidaceae and Pseudonocardioidaceae in the leaf endosphere of ryegrass compared with the control, which may be linked to the function of Nocardioidaceae in degrading a variety of organic compounds, including aromatic and polyaromatic pollutants and toxic chemicals.⁶³

Due to the differences in MP type and concentration, MPs can increase,⁶⁴ decrease,¹⁹ or neutrally influence⁶⁵ the Shannon diversity of soil microbial communities.

Under the existence of either PVC or PE in ryegrass soils, the addition of nano-Fe₃O₄ mediated the ryegrass microbiome in a different way: the plant bacterial community size and diversity were all enhanced in the phylloplane but weakened in the rhizoplane and rhizosphere soil.

In the ryegrass leaf endosphere, the bacterial diversity was significantly increased with PVC (+19%) and decreased with PE (−7%) under the addition of nano-Fe₃O₄. The plant microbiome is mainly derived from soils and is gradually enriched and filtered in various compartment niches.⁶⁶ Therefore, the observed effect of nano-Fe₃O₄ on the ryegrass root and leaf bacterial community structure can be mainly ascribed to its influence on the rhizosphere soil microbiome. This argument was also supported by the results from the structural equation model (SEM) shown in Figure 6. Moreover, the results demonstrated that the effect of nano-

470 Fe₃O₄ addition on the ryegrass bacterial community diversity
471 and structure varied under the PVC and PE treatments. This is
472 likely associated with the difference in the polymer backbone
473 structure of the two investigated MPs, as the polymer chemical
474 is an essential factor in modulating the responses of the
475 rhizosphere soil bacterial community functions, such as
476 carbohydrate metabolism, amino acid metabolism, and lipid
477 metabolism.⁶⁷ In terms of MP types, this study found that PE-
478 contaminated soils had greater plant rhizosphere bacterial
479 diversity than that of PVC-contaminated soils. This was
480 consistent with the study by Song et al., who compared the
481 effects of different MP types (biodegradable polylactide and
482 PVC) on plant (rice) rhizosphere bacterial communities.²⁰ In
483 the high-dose MP treatments (10% w/w), there were distinct
484 effects of MP types on the plant rhizosphere bacterial
485 communities (including diversity, community, and biomass),²⁰
486 although there were differences in plant species (rice versus
487 grass) and soil type (paddy field versus upland soils). The
488 present work further explored the effect of MPs on plant tissue
489 bacterial community structure and found a significant differ-
490 ence in the rhizoplane. The rhizoplane is a hotspot for
491 interactions between plants and MPs because MPs associate
492 with plant roots through attachment to root cap cells,
493 regardless of the MP size (either nano- or micro-sized
494 MPs).⁶⁸ Moreover, the effects of MPs on the plant microbiome
495 occur not only in plant roots but also in the plant phyllosphere,
496 which may be highly associated with the translocation/uptake
497 of MPs from plant roots to aboveground tissue, where MPs are
498 mostly aggregated on cell walls and in intercellular regions.⁶⁹

499 **Bacterial Co-occurrence Network.** In terms of com-
500 petitive/cooperative relationships, the above- and belowground
501 ryegrass bacterial microbiome exhibited co-occurrence pat-
502 terns, with positive correlations accounting for >60% of
503 potential interactions observed in the co-occurrence networks
504 of all treatments (Figure 5A). In the aboveground parts of the
505 plant, the positive associations in the ryegrass bacterial
506 microbiome were strengthened after the addition of nano-
507 Fe₃O₄ with PVC (from 70.6 to 79%) and PE (from 65.2 to
508 90%). Compared with the control with no chemical addition,
509 other treatments exhibited reduced belowground bacterial
510 positive interactions, as shown by the percentage of positive
511 links among the total interactions (78.2% in the control
512 compared to an average of 65.8% in other treatments). After
513 PE addition, the bacterial association was the least (60.5%);
514 however, combining PE with nano-Fe₃O₄ increased bacterial
515 interactions to 65% (Figure 5A).

516 A set of network topological parameters showed that the
517 ryegrass bacterial network complexity differed above and
518 belowground in response to the addition of MPs and nano-
519 Fe₃O₄ (Figure 5B). The addition of nano-Fe₃O₄ caused the
520 aboveground bacterial network to become more complex,
521 featuring a higher average path length and a greater degree of
522 centralization between nodes. The mediation of nano-Fe₃O₄
523 on MP was stronger for PVC than for PE. For example,
524 compared to the addition of PVC, the PE and nano-Fe₃O₄
525 treatment increased the aggregate structure of the below-
526 ground ryegrass bacterial network, as shown by the clustering
527 coefficient and centralization degree between nodes. The
528 average centralization degrees for the networks in all
529 treatments were distributed according to the power-law
530 distributions, demonstrating a nonrandom co-occurrence
531 pattern. Changes in the ryegrass bacterial network structure
532 could further affect network organizational principles such as

modularity. Thus, the nano network had the highest average
path length and diameter, but the highest modularity was
observed in the PE + nano treatment. Previous studies
reported the negative effects of MPs on the soil microbiome,
especially for bacterial communities.⁵⁷ Under the presence of
MPs, Fe₃O₄ NPs not only induced variation in bacterial
community structure but also had strong effects on co-
occurrence networks: the plant rhizosphere bacterial co-
occurrence relationships were strengthened by the addition
of NPs. The strengthened microbial functionality resilience
represents a potential of NPs for mitigating the negative effects
of MPs. In the present study, the addition of pure MPs induced
negative effects on the plant bacterial microbiome. This was
reported to be true even in larger soil microfood networks,
including soil bacteria, fungi, protists, and nematode
communities.⁷⁰ In agreement with Liu et al., in the present
work MPs decreased the stability of microbial- and microfood
networks,⁷⁰ with smaller MPs having stronger negative effects
than larger MPs. For ryegrass in this study, a minor dose effect
was observed for both the addition of NPs and MPs, which
could singly and jointly increase plant growth. However, a
previous study detected a strong MP dose effect in maize.⁷¹
The dose effect is most likely related to the plant type and
plant traits. For example, the MP dose effect was not obvious
for the ryegrass growth, but it was obvious for ryegrass
physiological and enzyme activities, which might have
profound ecological impacts on plant fitness, resulting in
uncertain consequences for ecosystems.⁷¹ In the present study,
the addition of pure Fe₃O₄ NPs showed a positive dose effect
on the plant microbiome through an increase in bacterial
keystone taxa and community associations. This could be
explained by the following advantages of Fe nanomaterials: (i)
Fe NPs have great potential due to their high adsorption
capacity and reactivity and (ii) nano-Fe facilitates rhizosphere
microbial changes, particularly in terms of the relative
abundances of dominant genera.¹⁶

In the present study, network analysis further confirmed the
negative influence of MPs in terms of undermining negative
and positive cohesion not only in soil but also in the plant
bacterial microbiome, indicating the destabilization of micro-
bial communities.⁷² Furthermore, the present results showed
that nano-Fe₃O₄ addition could mitigate the stress caused by
MP accumulation, improving ryegrass aboveground bacterial
abundance and creating communities dominated by positive
associations. The phenomenon may be linked with the
accumulation of the beneficial phyllosphere microbiome,
including N-fixing bacteria and pathogen-resistant microbes,
in improving plant performance.⁷³ Exogenous disturbances
such as MP pollutants lead to changes in the soil C:N ratio, as
indicated by the SEM (Figure 6), which are necessary resource
limitations for microbes.

**Combined Effects of Nano-Fe₃O₄ and MPs on
Ryegrass Microbiome.** The SEM showed that 22% of the
ryegrass bacterial microbiome (17% for the rhizosphere soil
microbiome) was explained by the selected key edaphic
variables (Figure 6). The ryegrass rhizosphere bacterial
microbiome was directly controlled by the soil indices, mainly
the pH ($R^2 = 0.61$), the C/N ratio ($R^2 = 0.39$), and plant
enzymes (SOD, POD, and MDA; $R^2 = 0.99$), while nano-
Fe₃O₄ and MPs affected the soil microbiome through soil
properties. The SEM analyses supported the observation that
nano-Fe₃O₄ and MPs had direct and positive correlations with
the soil pH and the C/N ratio (Table 1 and Figure 6). The

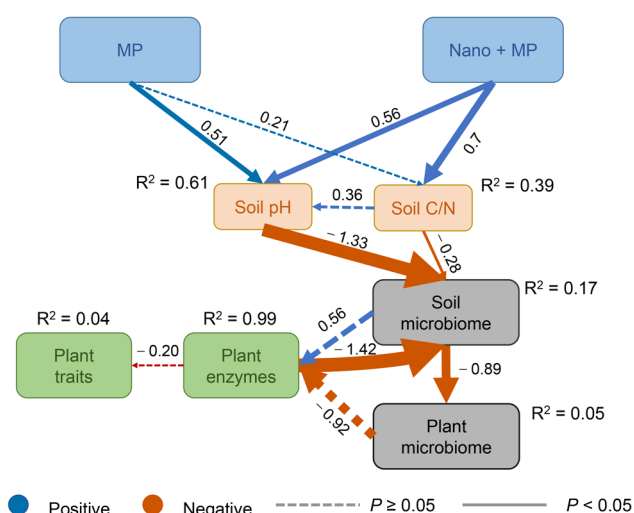


Figure 6. Structural equation model (SEM) showing the effects of nano-Fe₃O₄ and microplastics (MPs) on ryegrass rhizosphere soil properties (pH and C/N ratio), plant traits and enzymes, and plant and soil microbiomes. The numbers adjacent to the dashed (nonsignificant influence; $P > 0.05$) and solid (significant influence; $P < 0.05$) arrows are the standardized path coefficients. Arrow width indicates coefficient strength. Blue and red lines indicate positive and negative coefficients, respectively. R^2 indicates the proportion of variance in the ryegrass microbiome explained by the model.

the cross-talk mechanism of plant microbiome functionality (i.e., nutrient signaling and immune signaling), these changes in soil properties can finally affect the phyllosphere microbiome.⁷⁵ The connection between the phyllosphere microbiome and plant physiological activity can be explained by (i) alterations in the composition and activities of plant microbiomes that affect host functions⁷⁶ and (ii) the functional traits of the phyllosphere microbiome that mediate the hydraulic activation of stomata relevant to the foliar water uptake pathway.⁷⁵ The SEM in this work indicates significant microbial connectivity from the rhizosphere to the phylloplane. This association among different plant tissues can be largely attributed to the horizontal transmission of the microbiome, from the soil to the aboveground parts of the plant.⁷⁵ In addition to the bottom-up (soil–phyllosphere) effect, the foliar application of iron oxide NPs can also exert top-down effects through activating the antioxidative system, upregulating cytokinin synthesis, and promoting plant nutritional quality.³⁰ In terms of nanoenabled plant protection, the results showed a positive effect of nano-Fe₃O₄ from plant belowground soils. Moreover, Fe-based NP products can be applied by spraying them on the top of the soil as nanocarriers of biopesticides, which can weaken the toxicity of pesticides to soil microbiota.⁷⁷ NPs can also be applied as a foliar spray to enhance crop nutritional quality. These findings reflect the potential of NPs as an ecofriendly, high-efficiency, and sustainable plant protection strategy. With the development of advanced technologies, including inductively coupled plasma mass spectrometry, sensing techniques, and X-ray fluorescence imaging, research can deepen the understanding of the effects of NPs on plant–microbiome systems at the nanoscale—the scale of function in biology. It is anticipated that nanotechnologies coupled with metadata analytics could promote needs in plant microbiome research by analyzing microbial interactions at the relevant spatial (plant tissue) and temporal (plant growth) scales. On the other hand, MPs can concentrate in arable soils through plastic film breakage and atmospheric deposition. Under the long-term action of natural factors such as sun rays, rain, wind, and biodegradation, plastic waste would be disintegrated and form smaller MPs.⁷⁸ PE and PVC MPs have relatively high specific surface areas and hydrophobicity. The hydrophobic surface of MPs can be magnetized via binding nanoparticles.⁷⁹ Thus, in soil aqueous solution, numerous nano-Fe₃O₄ could be adhered on the MP surfaces under agricultural irrigation or humid conditions.

The PE and PVC MPs feature high mobility and strong affinity toward nano-Fe₃O₄ and other pollutants such as heavy metals and organic pollutants.^{37,80} The MP-adsorbed chemicals can be cotransported in soil, which would change the environmental fate and bioavailability of pollutants. Meanwhile, these chemicals can migrate downward in soil alongside MPs. In the process of practical application, pristine nano-Fe₃O₄ and MPs get added to soil but they can change dramatically over time, due to surface geochemical processes. The aging process can impact the MP mobility, adsorption capacity, and release of the associated contaminants derived from the MPs.^{37,80} In order to uncover the effects of aging on the release behavior of endogenous chemicals, the study on the release of chemicals from MPs and their interactions with nano-Fe₃O₄ should be strengthened. Our results showed nano-Fe₃O₄ mitigates the negative effects of MPs on the soil–microbe–plant system. By the application of exogenous nano-Fe₃O₄, massive MPs and their adhering pollutants can be

SEM results further indicated that pH had a significant ($P < 0.05$) and negative ($r = -1.33$) effect on variations in the bacterial microbiome, which was in accordance with the findings of previous studies. pH has been confirmed to be a predictor of the soil bacterial community.⁷⁴ The change in the plant microbiome was directly dependent on its rhizosphere soil bacterial microbiome ($R^2 = 0.05$), with 89% of the variation explained (Figure 6). Such findings emphasize the critical roles of soil in shaping the plant microbiome. In the controlled pot experiment, it was observed that nano-Fe₃O₄ mitigated the effect of MPs on the plant microbiome through the pathway of the rhizosphere soil properties to the plant rhizosphere and phyllosphere microbiome. As an open system, the phyllosphere is subjected to complex environmental perturbations, such as alterations in temperature, water availability, and light availability, which impact the crosstalk between plants and their microbiomes.⁷⁵ In the short term (years to decades), the adaptation of plants to environmental change is mainly driven by the plant microbiome.⁷⁶ In the present study, it was observed that the change in the plant microbiome was mainly dependent on its rhizosphere microbiome. However, the rhizosphere in natural soil is heterogeneous. The soil heterogeneity in a field scenario might weaken the observed significant trends from the homogenized system. Thus, subsequent long-term field experiments with considerations of single factors (environment or chemical) and their combined influences can be a promising way to capture detailed variations due to environmental and anthropogenic impacts.

The SEM results showed that the iron oxide NPs changed the plant rhizosphere soil properties and increased bacterial abundance. Plants form complex interaction networks with diverse microbiomes. Human-induced variation in soil environments shapes the nearby soil microbiome, and then, through

separated and removed by an environmentally friendly magnetic method.^{37,81} This is a promising way to mitigate the negative effects of MPs on agroecological systems.

CONCLUSION

Understanding how MP pollution impairs soil function and plant productivity is a priority topic within the general food security agenda. In this study, the use of nanoiron oxide soil amendments as a mechanism for mitigating plant stress effects arising from PE- and PVC-based MPs was explored in an experimental trial with *Lolium perenne*. The major strength of the present work is the comprehensive consideration of the plant microbiome, which spans the rhizosphere through the phylloplane. The addition of nano-Fe₃O₄ and MPs significantly affected the ryegrass rhizosphere environment and its surrounding soil microbiome, and such effects ultimately changed the plant microbiome. This study provides the evidence that nano-Fe₃O₄ can mitigate the negative effects of MPs on the ryegrass microbiome by (i) improving soil health (as revealed by the main soil quality indicators of the soil total carbon and C/N ratio) (ii) alleviating plant physiological stress and oxidative damage, (iii) promoting the bacterial abundance on leaf and root surfaces, especially taxa (such as Bacteroidetes and Firmicutes) that defend against environmental stresses, and (iv) strengthening the positive associations of the phyllosphere microbiome for potential pathogen resistance. In agricultural soils, MPs have high mobility and a hydrophobic surface with strong affinity for nanoparticles, and they can be magnetized via binding nanoparticles. Since the aging process can impact MP mobility and adsorption capacity, future investigations should focus on the plastic weathering and the interaction between MPs and nanomaterials. In total, the findings deepen the understanding of the impacts of MPs and the potential for nanomaterials to play a protective role and modulate the plant microbiome.

MATERIALS AND METHODS

Experimental Soil. Red soil is one of the most widespread soil types in China, with a total area of 56.9 million hectares. The soil was classified as a typical red sandy with a soil pH of 6.5 ± 0.01 , 19.97 ± 0.65 g kg⁻¹ total carbon content, 2.45 ± 0.21 g kg⁻¹ total N content, and 1.016 g cm⁻³ bulk density. Approximately 200 kg of MP-free homogeneous red soil was used for all of the pot experiments. Details on the soil texture, sampling site location, land-use background, and soil pretreatment can be found in the Supporting Information (SI). The soil pH of the suspension was measured using a pH meter (1:2.5 w/v soil-to-water ratio, Mettler-Toledo, Switzerland). Soil total carbon (TC) and total N (TN) were determined using an elementary analyzer-stable isotope ratio mass spectrometer (EI-IRMS; Elementar Vario PYRO cube and Isoprime100). The quality control (QC) of the soil pH test was achieved by performing replicate analysis of 10 samples in each batch test. The replicate results were set to fall within 0.1 pH unit, and analysis of one internal standard for every batch analysis was carried out. The acquired results were plotted in a quality control chart (QC chart) and monitored for Out of Warning Signals (± 2 sd). The QC of soil TC and TN data was assured by assessing each sample in 3 replicates to monitor the deviation under 5%. Blank samples (free of carbon and nitrogen), standard reference materials (China national certified reference soil: GSBZ50013-88), and duplicate samples were also applied in each batch of soil samples to control the quality of soil TC and TN.

The iron oxide content (Fe₂O₃) of soil samples was determined by converting the total Fe content into Fe₂O₃ content with the equation $\text{total Fe}_2\text{O}_3 \times 0.6993 = \text{total Fe}$. Soil total Fe content was determined by the inductively coupled plasma-atomic emission spectrometry

(ICP-AES) method after microwave digestion. The quality of total Fe content measured by the ICP-AES method was controlled by (i) testing all the samples 3 times (replicates to make sure the absolute deviation under the tolerance of China national standard (LY/T 1253-1999)), (ii) checking the internal standard (China national certified reference material (CRM): GBW (E) 070045) after every 10 samples (deviation less than 5%), (iii) interelement and background correction check sampling at the beginning, end, and at periodic intervals of every 10 samples throughout the sample run to ensure that deviation would within control limits, and (iv) plotting the results in a QC chart to ensure the linearity.

Experimental Setup. The pot experiment was laid out in a randomized block design in a greenhouse under natural light conditions at the KIB using five replications ($n = 5$). The position of each pot was changed three times during the experiment to homogenize the environmental conditions. In the greenhouse, the air temperature averaged 22.5 °C and the relative humidity averaged 40%. Pots (20 × 15 cm) were filled with a mixture of soil and compost at a ratio of 9:1 (total weight 2 kg) according to Freiberg et al.⁸² The compost used was commercial organic fertilizer specifically designed for pot plant growth (Gro-Rich COM, The Richlawn Company Organix Supply, USA). The treatments consisted of three exogenous chemical additives: PVC (Chemi Shanghai Aladdin Biochemical Technology Co. Ltd.; Chemical Abstracts Service number (CAS number 9002-86-2); (C₂H₃Cl)_n; 1.38 g/cm³; size ~100 μm), polyethylene (PE; Shanghai Aladdin Biochemical Technology Co. Ltd.; CAS number 25322-68-3; HO(CH₂CH₂O)_nH; 1.27 g/cm³; size ~75 μm; scanning electron micrographs and Fourier transform infrared (FTIR) spectra of PE and PVC particles are shown in Figure S4), and nano-Fe₃O₄ (20 nm in diameter; Shanghai Macklin Biochemical Technology Co. Ltd.; purity 99.5%; detailed dynamic light scattering (DLS) analysis and transmission-electron micrographs (TEM) of nano-Fe₃O₄ are shown in Figure S5). In total, 3 levels of nano-Fe concentrations (0%, 0.01%, and 0.05%) × 5 plastic treatments (0%, 1% PVC, 10% PVC, 1% PE, and 10% PE) = 15 treatments were used (Table S2). The 5 high dosing treatments (A, Control; C, 0.05% Nano; G, 10% PVC; I, 10% PVC + 0.05% Nano; M, 10% PE; O, 10% PE + 0.05% Nano) were selected for soil and microbial analyses. The details of MP pretreatment can be found in the SI. Soil OM was measured based on the national standard method (LY/T 1237-1999), whereas the Fe concentrations in both shoots and roots of ryegrass samples were measured using the ICP-AES method. The quality control of plant Fe concentrations was the same as that detecting Fe concentration in soils as described previously.

Perennial ryegrass (*Lolium perenne*) was chosen as a model species on the basis that it is the most widely grown cool-season grass worldwide and has been used widely for pot experiments.⁸³ The seeds were obtained from the Faculty of Animal Science and Technology, Yunnan Agricultural University. Around 500 ryegrass seeds were surface sterilized with 10% NaClO (5 min) and 75% ethanol (2 min) and then thoroughly rinsed with sterile water. The rinsed seeds were then germinated in sterilized sand trays, and 20 seedlings of similar size were subsequently transplanted into each pot. Deionized water (50 mL) was used to irrigate the pots every week to maintain the 50% water-holding capacity, while pesticides and fungicides were not used during the 90 day experimental period. The Fe concentrations in both shoots and roots in ryegrass samples were measured by using the ICP-AES method.

Plant Physiological Analysis. We collected fresh leaf samples and dark-stored them at 18 °C for chlorophyll analysis. A spectrophotometer was used to measure the chlorophyll A, chlorophyll B, and carotenoid concentrations (SPAD-502; Konica Minolta Sensing, Inc., Osaka, Japan). The chlorophyll concentrations were calculated by the following equations and expressed as the amount of chlorophyll g⁻¹ dry biomass:²⁵

$$\text{chlorophyll A: } 11.93 \times \lambda_{664\text{nm}} - 1.93 \times \lambda_{647\text{nm}}$$

$$\text{chlorophyll B: } 20.36 \times \lambda_{667\text{nm}} - 5.5 \times \lambda_{664\text{nm}}$$

The maximum quantum efficiency of photosystem II phytochemistry (Fv/Fm) was measured instantly on the adaxial ryegrass surface, according to Sharma et al.⁸⁴ Roots were manually collected and washed to remove the adhesion of soil particles. The plant height, root length, and fresh weight were measured, whereas the dry weight was determined by oven drying the samples at 50 °C for 12 h.²⁵ For plant chlorophyll A, chlorophyll B, carotenoid concentrations, and Fv/Fm, the QC contained the following steps: (i) calibrate spectrophotometers regularly using appropriate standards, (ii) include samples with internal standards and blank samples (solvent only) in each batch of plant samples, and (iii) analyze duplicate plant samples to assess the precision and repeatability. The activities of superoxide dismutase (SOD) and peroxidase (POD) in leaves and roots were determined by following the method of Li et al.⁸⁵ For SOD, POD, and MDA activity measurement in leaf and root samples, the QC contained the following steps: (i) test and analyze duplicate plant samples (3 times) to assess the precision and repeatability of the enzyme activity determination, (ii) use certified reference materials with known enzyme activity levels to validate the accuracy, and (iii) create control charts to monitor the performance of the testing method over time.

Plant Microbiome DNA Extractions. Destructive samplings were conducted at the plant maturing stage (80 days after sowing). For the rhizosphere, the soil adhering to the root was gently shaken off and collected (10 g) in a sterile tube.⁶⁶ The roots and leaves were rinsed three times with sterile water. Root and leaf samples (50 g) were placed into a centrifuge tube (50 mL) containing buffer (1 M Tris-HCl, 0.5 M Na₂EDTA, 1.2% CTAB, pH = 8) and then centrifuged (5 min at 4000g). The vortexed liquid was filtered (0.22 μm) to collect microbes from phylloplane and rhizoplane samples. MP Fast DNA spin kit (MP Biomedicals, Solon, OH, USA) was used to collect the microbial cells and extract epiphytic DNA based on the method of Ruiz-Perez et al.⁸⁶ Before subsequent endophytes (leaf endosphere and root endosphere) DNA extraction, the disinfection was verified (from the same leaves and roots) by adding the 100 μL last rinse sterile water to the PDA, LB, and Gao's No. 1 culture media.^{66,86} Sterilized leaves and roots were pulverized using a Mixer Mill (MM400, Retsch, Germany), and endophytic DNA was extracted using a Power Soil DNA kit (MoBio, Carlsbad, CA, USA). PowerSoil DNA isolation kit was also used to extract DNA from rhizosphere soils (0.5 g). The DNA quality was checked by agarose gel (2%) electrophoresis. The DNA concentration and purity were measured using a NanoDrop 2000C spectrophotometer (Thermo Scientific, Wilmington, USA.).

Quantitative PCR and Illumina Amplicon Sequencing. Quantitative real-time PCR (qPCR) was conducted using primer pairs 338F/806R to quantify gene copy numbers of bacterial communities from five compartment niches of ryegrass. The qPCR reaction mix contained qPCR Supermix (5 μL), primer (0.5 μL), template DNA (1 μL), and ddH₂O (3 μL). To estimate bacterial gene abundances, a standard curve was generated with a 10-fold serial dilution of a plasmid template in which the target gene amplified from the sample had been ligated to the T-vector (pMD18-T). Fluorescence intensities were detected in an Analytikjena-qTOWER2 instrument (Analytik, Jena, Germany) with the following cycling conditions: 94 °C for 3 min, 39 cycles of 20 s at 94 °C, 63 °C 30 s, and 72 °C 30 s. Each plant and soil DNA (biological replicates) was subjected to three independent qPCR runs (technical replicates), and the final gene copy number (copies/μL) was calculated from the 880 equation

$$\begin{aligned} \text{gene copy number} &= \text{plasmid concentration of standard} \\ &\times 6.02 \times 10^{23} \\ &/ (\text{length of target segment} + \text{vector}) \\ &\times 1 \times 10^9 \times 660 \end{aligned}$$

For the microbial DNA, Illumina amplicon sequencing of V3–V4 (hypervariable region of the bacterial 16S rRNA) was performed using the primer pairs 338F/806R.⁸⁷ PCR reaction mix contained

ddH₂O (10 μL), primer (10 μM), High GC Enhancer (10 μL), dNTP (10 μL), Q5 High-Fidelity DNA Polymerase (0.2 μL), and template DNA (60 ng). PCR thermal cycling conditions were as follows: 95 °C for 5 min (initial denaturation), 15 cycles of 60 s at 95 °C, 50 °C 60 s, and 72 °C 60 s, concluded with a final extension for 7 min at 72 °C. Amplicons were purified with VAHTSTM DNA Clean Beads, and DNA concentrations were measured with a Nanodrop 2000 instrument (Thermo Scientific, Wilmington, DE, USA) and quantified by QuantiT dsDNA HS Reagent. Purified amplicons were combined in equimolar concentrations and sequenced (2 × 250 paired ends) on the Illumina PE250 platform. Obtained sequences were demultiplexed on the QME2 platform and stitched using FLASH2. DADA 2 software was used to denoise and dereplicate reads. The remaining reads were denoted as amplicon sequence variants (ASVs) by searching effective reads against the SILVA-based bacteria reference alignment (version 128). To minimize the impact of read count variation from different samples, the number of sequences for each sample was then normalized, randomly subsampling them to the sample with the minimum read count. All sequence data have been deposited in the Sequence Read Archive under accession number PRJNA916371.

Statistical Analysis. Soil and plant traits were presented as the mean standard error. Analysis of variance (one-way ANOVA) with an associated least significant difference (LSD) test at a 5% probability level was used to test the significant difference among treatments for plant physiological and bacterial communities among plant compartments and/or chemical treatments. All of the statistical analyses were performed in the R environment (version 3.60). Alpha-diversity difference of plant bacterial communities was estimated using the Shannon diversity index based on ASVs. Plant bacterial community structure (beta-diversity) was evaluated by pairwise Bray–Curtis distances and visualized using principal coordinate analysis (PCoA) plots. Permutational multivariate analysis of variance (PERMANOVA) was applied to test the significant differences of the ryegrass-associated bacterial community in different compartments using the Adonis function of the R package *vegan* v2.6-1. The random forest analysis by bootstrapping and the nonparametric test was applied to identify the significantly different biomarkers at the family level of different Nano and MP additions. Mean Decrease Gini was selected as the indicator value in the analysis using the “trans_diff class” function of the R package *microeco* v0.90. Co-occurrence network analyses of bacterial taxa from aboveground (leaf endophyte and phylloplane) and belowground (root endosphere, rhizoplane, and rhizosphere soil) were examined separately in the R environment with *igraph*, *psych*, and *microeco* packages,⁸⁸ following the protocols described by Barberan et al.⁸⁹ To reduce the network's complexity, we only examined strong interactions between different genera with $p < 0.05$ and Spearman's $\rho > 0.80$, and the p values were adjusted using the Benjamini–Hochberg (FDR) method. All strong correlations identified from a pairwise comparison of genus abundance formed a correlation network in which the node represented bacterial genus taxa, and the edge represented a strong and significant correlation between the nodes. The network was visualized in Gephi (version 0.9.2; <https://gephi.org/>) with a Fruchterman–Reingold layout algorithm. The network complexity was defined by a series of topological parameters (number of nodes and edges, average path length, network diameter, centralisation degree, average degree, clustering coefficient, and modularity) calculated in R package *igraph*. Structural equation modeling (SEM) analysis was conducted using the *lavaan* R package (version 0.60) to evaluate the direct and indirect effects of MP and nano-Fe₃O₄ addition on plant and soil microbiomes. We considered a hypothesized conceptual model (Figure S3) that included all reasonable pathways. The vector “MP” indicated the treatment with PE and PVC addition (“0” for nonaddition and “1” for PE or PVC addition). The vector “MP + nano-Fe₃O₄” indicated the treatments with PE/PVC and Nano addition (“0” for nonaddition and “1” for PE + Nano or PVC + nano-Fe₃O₄ addition). The vector “Soil microbiome” indicated the Shannon index of the soil bacterial communities from different treatments. All variables besides “MP” and “MP + Nano” were 953

standardized by log10 transformation to improve normality in R. A principal component analysis (PCA) was applied to simplify the variables of “Plant microbiome”, “Plant enzymes”, and “Plant traits” subjected to SEM. Specifically, “Plant microbiome” was represented by the PCA axis (PCA1), explaining 35% of the variation in the Shannon index of rhizosphere, root endosphere, leaf endosphere, and phylloplane bacterial communities. “Plant enzymes” was represented by the PCA1, explaining 37% of the variation in the three leaf and root enzyme activities. “Plant traits” was represented by the PCA1 explaining 49% of the variation in plant height, root length, fresh weight, dry weight, aboveground biomass, chlorophyll A content, chlorophyll B content, chlorophyll, and carotenoid content. Then, we sequentially eliminated nonsignificant pathways unless the pathways were biologically informative.

ASSOCIATED CONTENT

Supporting Information

The Supporting Information is available free of charge at <https://pubs.acs.org/doi/10.1021/acsnano.3c05809>.

Permutational multivariate analysis of variance in soil bacterial communities, overall experimental design, random forest analysis of significant taxonomical changes in plant, conceptual model of structural equation model, background of agricultural soil, microplastic pretreatment and dosing section, and plant physiological analysis (PDF)

AUTHOR INFORMATION

Corresponding Author

Heng Gui – Department of Economic Plants and Biotechnology, Yunnan Key Laboratory for Wild Plant Resources, Kunming Institute of Botany and Centre for Mountain Futures (CMF), Kunming Institute of Botany, Chinese Academy of Sciences, Kunming 650201, People's Republic of China; Email: guiheng@mail.kib.ac.cn

Authors

Dong Liu – The Germplasm Bank of Wild Species, Yunnan Key Laboratory for Fungal Diversity and Green Development, Kunming Institute of Botany, Chinese Academy of Sciences, Kunming 650201 Yunnan, People's Republic of China

Shahid Iqbal – Department of Economic Plants and Biotechnology, Yunnan Key Laboratory for Wild Plant Resources, Kunming Institute of Botany and Centre for Mountain Futures (CMF), Kunming Institute of Botany, Chinese Academy of Sciences, Kunming 650201, People's Republic of China

Jianchu Xu – Department of Economic Plants and Biotechnology, Yunnan Key Laboratory for Wild Plant Resources, Kunming Institute of Botany and Centre for Mountain Futures (CMF), Kunming Institute of Botany, Chinese Academy of Sciences, Kunming 650201, People's Republic of China

Shaoshan An – State Key Laboratory of Soil Erosion and Dryland Farming on the Loess Plateau, Institute of Soil and Water Conservation, Northwest A&F University, Yangling 712100, People's Republic of China

Baoshan Xing – Stockbridge School of Agriculture, University of Massachusetts, Amherst, Massachusetts 01003, United States

Complete contact information is available at:
<https://pubs.acs.org/doi/10.1021/acsnano.3c05809>

Notes

The authors declare no competing financial interest.

ACKNOWLEDGMENTS

This study was supported by the Strategic Priority Research Program of the Chinese Academy of Sciences (Grant Nos. XDA26020203 and XDA26050302). We also acknowledge support from the National Natural Science Foundation of China (NSFC Grant No. 32371785) and the Youth Innovation Promotion Association of CAS, China (Grant No. 2022396). D.L. acknowledges funding from the Yunnan Revitalization Talent Support Program “Young Talent” Project (YNQR-QNRC-2019-025). S.I. acknowledges funding from the Postdoctoral Directional Training Foundation of Yunnan (Grant No. EO3A581261) and CAS-President's International Fellowship Initiative (2021PB00094). We thank LetPub (www.letpub.com) for its linguistic assistance during the preparation of this manuscript.

REFERENCES

- (1) Ingrassia, R.; Amato, G.; Bagarello, V.; Carollo, F. G.; Giambalvo, D.; Iovino, M.; Lehmann, A.; Rillig, M. C.; Frenda, A. S. Polyester microplastic fibers affect soil physical properties and erosion as a function of soil type. *Soil* **2022**, *8*, 421–435.
- (2) Chauhan, S. S.; Singh, J. K.; Singh, H.; Mavi, S.; Singh, V.; Khan, M. I. An overview on recycling plastic wastes in bricks. *Materials Today: Proceedings* **2021**, *47*, 4067–4073.
- (3) Yadav, H.; Khan, M. R. H.; Quadir, M.; Rusch, K. A.; Mondal, P. P.; Orr, M.; Xu, E. G.; Iskander, S. M. Cutting boards: An overlooked source of microplastics in human food? *Environ. Sci. Technol.* **2023**, *57* (22), 8225–8235.
- (4) Zhang, J.; Ma, C.; Xia, X.; Li, Y.; Lin, X.; Zhang, Y.; Yang, Z. Differentially charged nanoplastics induce distinct effects on the growth and gut of benthic insects (*chironomus kiinensis*) via charge-specific accumulation and perturbation of the gut microbiota. *Environ. Sci. Technol.* **2023**, *57* (30), 11218–11230.
- (5) Xu, Y.; Zeng, L.; Tao, Y.; Xu, J.; He, Y.; Lu, Z. Release of additives from agricultural plastic films in water: Experiment and modeling. *Environ. Sci. Technol.* **2023**, *57* (27), 10053–10061.
- (6) Pham, D. T.; Kim, J.; Lee, S. H.; Kim, J.; Kim, D.; Hong, S.; Jung, J.; Kwon, J. H. Analysis of microplastics in various foods and assessment of aggregate human exposure via food consumption in Korea. *Environ. Pollut.* **2023**, *322*, No. 121153.
- (7) Zhang, K.; Yang, J.; Chen, L.; He, J.; Qu, D.; Zhang, Z.; Liu, Y.; Li, X.; Liu, J.; Li, J.; Xie, X.; Wang, Q. Gut microbiota participates in polystyrene microplastics-induced hepatic injuries by modulating the gut–liver axis. *ACS Nano* **2023**, *17* (15), 15125–15145.
- (8) Wang, C.; Song, X.; Li, T.; Zhu, X.; Yang, S.; Zhu, J.; He, X.; Gao, J.; Xu, H. Biodegradable electroactive nanofibrous air filters for long-term respiratory healthcare and self-powered monitoring. *ACS Appl Mater Inter* **2023**, *15* (31), 37580–37592.
- (9) Hofmann, T.; Ghoshal, S.; Tufenkji, N.; Adamowski, J. F.; Bayen, S.; Chen, Q.; Demokritou, P.; Flury, M.; Hüffer, T.; Ivleva, N. P.; Ji, R.; Leask, R. L.; Maric, M.; Mitran, D. M.; Sander, M.; Pahl, S.; Rillig, M. C.; Walker, T. R.; White, J. C.; Wilkinson, K. J. Plastics can be used more sustainably in agriculture. *Commun Earth Environ* **2023**, *4* (1), No. 332.
- (10) Huang, Y.; Liu, Q.; Jia, W. Q.; Yan, C. R.; Wang, J. Agricultural plastic mulching as a source of microplastics in the terrestrial environment. *Environ. Pollut.* **2020**, *260*, No. 114096.
- (11) Akhir, M. A. M.; Mustapha, M. Formulation of biodegradable plastic mulch film for agriculture crop protection: A review. *Polym Rev* **2022**, *62* (4), 890–918.
- (12) Kasirajan, S.; Ngouajio, M. Polyethylene and biodegradable mulches for agricultural applications: a review. *Agron Sustain Dev* **2012**, *32* (2), 501–529.

- (13) Iqbal, S.; Xu, J.; Allen, S. D.; Khan, S.; Nadir, S.; Arif, M. S.; Yasmeen, T. Unraveling consequences of soil micro-and nano-plastic pollution on soil-plant system: Implications for nitrogen (N) cycling and soil microbial activity. *Chemosphere* **2020**, *260*, No. 127578.
- (14) Lehmann, A.; Leifheit, E. F.; Gerdawischke, M.; Rillig, M. C. Microplastics have shape- and polymer-dependent effects on soil aggregation and organic matter loss—an experimental and meta-analytical approach. *Micropla Nanopla* **2021**, *1* (1), 1–14.
- (15) Bosker, T.; Bouwman, L. J.; Brun, N. R.; Behrens, P.; Vijver, M. G. Microplastics accumulate on pores in seed capsule and delay germination and root growth of the terrestrial vascular plant *Lepidium sativum*. *Chemosphere* **2019**, *226*, 774–781.
- (16) Liu, Y. Y.; Cui, W. Z.; Li, W. G.; Xu, S.; Sun, Y. H.; Xu, G. J.; Wang, F. Y. Effects of microplastics on cadmium accumulation by rice and arbuscular mycorrhizal fungal communities in cadmium-contaminated soil. *J Hazard Mater* **2023**, *442*, No. 130102.
- (17) Sun, Y.; Li, X.; Cao, N.; Duan, C.; Ding, C.; Huang, Y.; Wang, J. Biodegradable microplastics enhance soil microbial network complexity and ecological stochasticity. *J Hazard Mater* **2022**, *439*, No. 129610.
- (18) Ding, L.; Zhang, S. Y.; Wang, X. Y.; Yang, X. M.; Zhang, C. T.; Qi, Y. B.; Guo, X. T. The occurrence and distribution characteristics of microplastics in the agricultural soils of Shaanxi Province, in north-western China. *Sci. Total Environ.* **2020**, *720*, No. 137525.
- (19) Fei, Y.; Huang, S.; Zhang, H.; Tong, Y.; Wen, D.; Xia, X.; Wang, H.; Luo, Y.; Barceló, D. J. Response of soil enzyme activities and bacterial communities to the accumulation of microplastics in an acid cropped soil. *Sci. Total Environ.* **2020**, *707*, No. 135634.
- (20) Song, B.; Shang, S.; Cai, F. M.; Liu, Z.; Fang, J.; Li, N.; Adams, J. M.; Razavi, B. S. Microbial resistance in rhizosphere hotspots under biodegradable and conventional microplastic amendment: Community and functional sensitivity. *Soil Biol Biochem* **2023**, *180*, No. 108989.
- (21) de Souza Machado, A. A.; Lau, C. W.; Kloas, W.; Bergmann, J.; Bachelier, J. B.; Faltin, E.; Becker, R.; Gorlich, A. S.; Rillig, M. C. Microplastics can change soil properties and affect plant performance. *Environ. Sci. Technol.* **2019**, *53* (10), 6044–6052.
- (22) Lei, C.; Engeseth, N. J. Comparison of growth and quality between hydroponically grown and soil-grown lettuce under the stress of microplastics. *ACS ES&T Water* **2022**, *2* (7), 1182–1194.
- (23) Iqbal, S.; Xu, J.; Khan, S.; Arif, M. S.; Yasmeen, T.; Nadir, S.; Schaefer, D. A. Deciphering microplastic ecotoxicology: impacts on crops and soil ecosystem functions. *Cir Agr Sys* **2021**, *1* (1), 1–7.
- (24) Xiao, F.; Zhang, S.; Yan, Z.; Liu, Y.; Ming, Y.; Li, N.; Lai, Y.; Liu, M.; Wang, Y. Effects of microplastics on plant performance of invasive species *Phytolacca americana* and its non-invasive congeners. *SSRN* **2022**, No. 4312938.
- (25) Boots, B.; Russell, C. W.; Green, D. S. Effects of microplastics in soil ecosystems: above and below ground. *Environ. Sci. Technol.* **2019**, *53* (19), 11496–11506.
- (26) Bengtsson, J.; Bullock, J.; Egoh, B.; Everson, C.; Everson, T.; O'Connor, T.; O'Farrell, P.; Smith, H.; Lindborg, R. Grasslands more important for ecosystem services than you might think. *Ecosphere* **2019**, *10* (2), No. e02582.
- (27) Bhaskar, M.; Kumar, A.; Rani, R. Application of nano formulations in agriculture. *Biocata Agricul Biotechnol* **2023**, *54*, No. 102934.
- (28) Cao, X.; Wang, C.; Luo, X.; Yue, L.; White, J. C.; Elmer, W.; Dhankher, O. P.; Wang, Z.; Xing, B. Elemental sulfur nanoparticles enhance disease resistance in tomatoes. *ACS Nano* **2021**, *15* (7), 11817–11827.
- (29) Wang, C.; Ji, Y.; Cao, X.; Yue, L.; Chen, F.; Li, J.; Yang, H.; Wang, Z.; Xing, B. Carbon dots improve nitrogen bioavailability to promote the growth and nutritional quality of soybeans under drought stress. *ACS Nano* **2022**, *16* (8), 12415–12424.
- (30) Cao, X.; Yue, L.; Wang, C.; Luo, X.; Zhang, C.; Zhao, X.; Wu, F.; White, J. C.; Wang, Z.; Xing, B. Foliar application with iron oxide nanomaterials stimulate nitrogen fixation, yield, and nutritional quality of soybean. *ACS Nano* **2022**, *16* (1), 1170–1181.
- (31) Wang, Z.; Yue, L.; Dhankher, O. P.; Xing, B. S. Nano-enabled improvements of growth and nutritional quality in food plants driven by rhizosphere processes. *Environ Int* **2020**, *142*, No. 105831.
- (32) Xu, J.; Chen, Y.; Luo, J.; Xu, J.; Zhou, G.; Yu, Y.; Xue, L.; Yang, L.; He, S. Fe₃O₄ nanoparticles affect paddy soil microbial-driven carbon and nitrogen processes: roles of surface coating and soil types. *Environ Sci-Nano* **2022**, *9* (7), 2440–2452.
- (33) Tombuloglu, H.; Slimani, Y.; Tombuloglu, G.; Almessiere, M.; Baykal, A. Uptake and translocation of magnetite (Fe₃O₄) nanoparticles and its impact on photosynthetic genes in barley (*Hordeum vulgare* L.). *Chemosphere* **2019**, *226*, 110–122.
- (34) Zhang, W.; Jia, X.; Chen, S.; Wang, J.; Ji, R.; Zhao, L. J. Response of soil microbial communities to engineered nanomaterials in presence of maize (*Zea mays* L.) plants. *Environ. Pollut.* **2020**, *267*, No. 115608.
- (35) He, S.; Feng, Y.; Ren, H.; Zhang, Y.; Gu, N.; Lin, X. J. The impact of iron oxide magnetic nanoparticles on the soil bacterial community. *J Soil Sediment* **2011**, *11* (8), 1408–1417.
- (36) Rashid, M. I.; Shahzad, T.; Shahid, M.; Imran, M.; Dhavamani, J.; Ismail, I. M.; Basahi, J. M.; Almeelbi, T. J. Toxicity of iron oxide nanoparticles to grass litter decomposition in a sandy soil. *Sci Rep* **2017**, *7* (1), 1–11.
- (37) Shi, X.; Zhang, X.; Gao, W.; Zhang, Y.; He, D. Removal of microplastics from water by magnetic nano-Fe₃O₄. *Sci. Total Environ.* **2022**, *802*, No. 149838.
- (38) Yang, W.; Cheng, P.; Adams, C. A.; Zhang, S.; Sun, Y.; Yu, H.; Wang, F. Effects of microplastics on plant growth and arbuscular mycorrhizal fungal communities in a soil spiked with ZnO nanoparticles. *Soil Biol Biochem* **2021**, *155*, No. 108179.
- (39) Xu, B. L.; Liu, F.; Cryder, Z.; Huang, D.; Lu, Z. J.; He, Y.; Wang, H. Z.; Lu, Z. M.; Brookes, P. C.; Tang, C. X.; Gan, J.; Xu, J. M. Microplastics in the soil environment: Occurrence, risks, interactions and fate - A review. *Crit Rev Env Sci Tec* **2020**, *50* (21), 2175–2222.
- (40) Zeng, F. R.; Ali, S.; Zhang, H. T.; Ouyang, Y. B.; Qiu, B. Y.; Wu, F. B.; Zhang, G. P. The influence of pH and organic matter content in paddy soil on heavy metal availability and their uptake by rice plants. *Environ. Pollut.* **2011**, *159* (1), 84–91.
- (41) Lozano, Y. M.; Lehnert, T.; Linck, L. T.; Lehmann, A.; Rillig, M. C. Microplastic shape, polymer type, and concentration affect soil properties and plant biomass. *Front Plant Sci* **2021**, *12*, No. 714541.
- (42) Fan, J.; Liu, F.; Hu, Y. D.; Chen, J. W. Effects of pH and ionic composition on sorption/desorption of natural organic matter on zero-valent iron and magnetite nanoparticles. *Water Sci. Technol.* **2015**, *72* (2), 303–310.
- (43) Moore, O. W.; Curti, L.; Woules, C.; Bradley, J. A.; Babakhani, P.; Mills, B. J. W.; Homoky, W. B.; Xiao, K. Q.; Bray, A. W.; Fisher, B. J.; Kazemian, M.; Kaulich, B.; Dale, A. W.; Peacock, C. L. Long-term organic carbon preservation enhanced by iron and manganese. *Nature* **2023**, *621*, 312.
- (44) Zhao, T.; Fang, M.; Tang, Z.; Zhao, X.; Xie, F.; Wu, F.; Giesy, J. P. Effects of fulvic acid on aggregation, sedimentation, and adsorption of Fe₃O₄ magnetic nanoparticles. *Environ Sci Pollut R* **2019**, *26* (21), 21463–21474.
- (45) Lowry, G. V.; Avellan, A.; Gilbertson, L. M. Opportunities and challenges for nanotechnology in the agri-tech revolution. *Nature Nanotechnology* **2019**, *14* (6), 517–522.
- (46) Wang, J.; Cao, X.; Wang, C.; Chen, F.; Feng, Y.; Yue, L.; Wang, Z.; Xing, B. Fe-based nanomaterial-induced root nodulation is modulated by flavonoids to improve soybean (*Glycine max*) growth and quality. *ACS Nano* **2022**, *16* (12), 21047–21062.
- (47) Sabet, H.; Mortazaeinezhad, F. Yield, growth and Fe uptake of cumin (*Cuminum cyminum* L.) affected by Fe-nano, Fe-chelated and Fe-siderophore fertilization in the calcareous soils. *J Trace Elem Med Bio* **2018**, *50*, 154–160.
- (48) Rahemi, M.; Gharechahi, S. R.; Sedaghat, S. The application of nano-iron chelate and iron chelate to soil and as foliar application: Treatments against chlorosis and fruit quality in quince. *Int J Fruit Sci* **2020**, *20* (3), 300–313.

- (49) Liang, G. Iron uptake, signaling, and sensing in plants. *Plant Communications* **2022**, 3 (5), No. 100349.
- (50) Iqbal, S.; Xu, J.; Khan, S.; Arif, M. S.; Allen, S. D.; et al. Deciphering microplastic ecotoxicology: impacts on crops and soil ecosystem functions. *Circ Agri Sys* **2021**, 1 (8), 1–7.
- (51) Zhang, W.; Jia, X.; Chen, S.; Wang, J.; Ji, R.; Zhao, L. Response of soil microbial communities to engineered nanomaterials in presence of maize (*Zea mays* L.) plants. *Environ. Pollut.* **2020**, 267, No. 115608.
- (52) Zhao, T. T.; Lozano, Y. M.; Rillig, M. C. Microplastics increase soil pH and decrease microbial activities as a function of microplastic shape, polymer type, and exposure time. *Front Env Sci* **2021**, 9, No. 675803.
- (53) Liu, H. F.; Yang, X. M.; Liu, G. B.; Liang, C. T.; Xue, S.; Chen, H.; Ritsema, C. J.; Geissen, V. Response of soil dissolved organic matter to microplastic addition in Chinese loess soil. *Chemosphere* **2017**, 185, 907–917.
- (54) Dong, B.; Sang, W. L.; Jiang, D. X.; Zhou, J. M.; Kong, F. X.; Hu, W.; Wang, L. S. Effects of aluminum on physiological metabolism and antioxidant system of wheat (*Triticum aestivum* L.). *Chemosphere* **2002**, 47 (1), 87–92.
- (55) Gao, M. L.; Liu, Y.; Song, Z. G. Effects of polyethylene microplastic on the phytotoxicity of di-n-butyl phthalate in lettuce (*Lactuca sativa* L. var. *ramosa* Hort). *Chemosphere* **2019**, 237, 124482.
- (56) Liu, Y.; Kornig, C.; Qi, B.; Schmutzler, O.; Staufer, T.; Sanchez-Cano, C.; Magel, E.; White, J. C.; Feliu, N.; Gruner, F.; Parak, W. J. Size- and ligand-dependent transport of nanoparticles in matricaria chamomilla as demonstrated by mass spectroscopy and x-ray fluorescence imaging. *ACS Nano* **2022**, 16 (8), 12941–12951.
- (57) Zhu, D.; Ma, J.; Li, G.; Rillig, M. C.; Zhu, Y. G. Soil plastispheres as hotpots of antibiotic resistance genes and potential pathogens. *ISME J* **2022**, 16 (2), 521–532.
- (58) Lozano, Y. M.; Lehnert, T.; Linck, L. T.; Lehmann, A.; Rillig, M. C. Microplastic shape, polymer type, and concentration affect soil properties and plant biomass. *Front Plant Sci* **2021**, 12, No. 714541.
- (59) Liu, D.; Keiblinger, K. M.; Schindlbacher, A.; Wegner, U.; Sun, H. Y.; Fuchs, S.; Lassek, C.; Riedel, K.; Zechmeister-Boltenstern, S. Microbial functionality as affected by experimental warming of a temperate mountain forest soil-A metaproteomics survey. *Appl Soil Ecol* **2017**, 117, 196–202.
- (60) Turner, T. R.; James, E. K.; Poole, P. S. The plant microbiome. *Genome Biol* **2013**, 14 (6), No. 209.
- (61) Monteiro, R. A.; Balsanelli, E.; Wasseem, R.; Marin, A. M.; Brusamarello-Santos, L. C. C.; Schmidt, M. A.; Tadra-Sfeir, M. Z.; Pankiewicz, V. C. S.; Cruz, L. M.; Chubatsu, L. S.; Pedrosa, F. O.; Souza, E. M. Herbaspirillum-plant interactions: microscopical, histological and molecular aspects. *Plant Soil* **2012**, 356 (1–2), 161–175.
- (62) Liu, D.; Cai, J.; He, H. J.; Yang, S. M.; Chater, C. C. C.; Yu, F. Q. Anemochore seeds harbor distinct fungal and bacterial abundance, composition, and functional profiles. *J Fungi* **2022**, 8 (1), 89.
- (63) Zhang, H. L.; Huang, M.; Zhang, W. H.; Gardea-Torresdey, J. L.; White, J. C.; Ji, R.; Zhao, L. J. Silver nanoparticles alter soil microbial community compositions and metabolite profiles in unplanted and cucumber-planted soils. *Environ. Sci. Technol.* **2020**, 54 (6), 3334–3342.
- (64) Ren, X. W.; Tang, J. C.; Liu, X. M.; Liu, Q. L. Effects of microplastics on greenhouse gas emissions and the microbial community in fertilized soil. *Environ. Pollut.* **2020**, 256, No. 113347.
- (65) Wang, J.; Liu, X.; Dai, Y.; Ren, J.; Li, Y.; Wang, X.; Zhang, P.; Peng, C. Effects of co-loading of polyethylene microplastics and ciprofloxacin on the antibiotic degradation efficiency and microbial community structure in soil. *Sci. Total Environ.* **2020**, 741, No. 140463.
- (66) Xiong, C.; Zhu, Y. G.; Wang, J. T.; Singh, B.; Han, L. L.; Shen, J. P.; Li, P. P.; Wang, G. B.; Wu, C. F.; Ge, A. H.; Zhang, L. M.; He, J. Z. Host selection shapes crop microbiome assembly and network complexity. *New Phytol* **2021**, 229 (2), 1091–1104.
- (67) Sun, Y. Z.; Duan, C. X.; Cao, N.; Li, X. F.; Li, X. M.; Chen, Y. M.; Huang, Y.; Wang, J. Effects of microplastics on soil microbiome: The impacts of polymer type, shape, and concentration. *Sci. Total Environ.* **2022**, 806, No. 150516.
- (68) Taylor, S. E.; Pearce, C. I.; Sanguinet, K. A.; Hu, D.; Chrisler, W. B.; Kim, Y. M.; Wang, Z.; Flury, M. Polystyrene nano- and microplastic accumulation at *Arabidopsis* and wheat root cap cells, but no evidence for uptake into roots. *Environmental Science: Nano* **2020**, 7 (7), 1942–1953.
- (69) Liu, Y.; Guo, R.; Zhang, S.; Sun, Y.; Wang, F. Uptake and translocation of nano/microplastics by rice seedlings: Evidence from a hydroponic experiment. *J Hazard Mater* **2022**, 421, No. 126700.
- (70) Liu, M.; Wang, C.; Zhu, B. Drought alleviates the negative effects of microplastics on soil micro-food web complexity and stability. *Environ. Sci. Technol.* **2023**, 57 (30), 11206–11217.
- (71) Yang, W.; Cheng, P.; Adams, C. A.; Zhang, S.; Sun, Y.; Yu, H.; Wang, F. Effects of microplastics on plant growth and arbuscular mycorrhizal fungal communities in a soil spiked with ZnO nanoparticles. *Soil Biol Biochem* **2021**, 155, No. 108179.
- (72) Hernandez, D. J.; David, A. S.; Menges, E. S.; Searcy, C. A.; Afkhami, M. E. Environmental stress destabilizes microbial networks. *ISME J* **2021**, 15 (6), 1722–1734.
- (73) Zhan, C.; Matsumoto, H.; Liu, Y.; Wang, M. Pathways to engineering the phyllosphere microbiome for sustainable crop production. *Nat Food* **2022**, 3 (12), 997–1004.
- (74) Lauber, C. L.; Hamady, M.; Knight, R.; Fierer, N. Pyrosequencing-based assessment of soil pH as a predictor of soil bacterial community structure at the continental scale. *Appl Environ Microb* **2009**, 75 (15), 5111–5120.
- (75) Zhu, Y. G.; Xiong, C.; Wei, Z.; Chen, Q. L.; Ma, B.; Zhou, S. Y.; Tan, J.; Zhang, L. M.; Cui, H. L.; Duan, G. L. Impacts of global change on the phyllosphere microbiome. *New Phytol* **2022**, 234 (6), 1977–1986.
- (76) Trivedi, P.; Batista, B. D.; Bazany, K. E.; Singh, B. K. Plant-microbiome interactions under a changing world: responses, consequences and perspectives. *New Phytol* **2022**, 234 (6), 1951–1959.
- (77) Pontes, M. S.; Santos, J. S.; da Silva, J. L.; Miguel, T.; Miguel, E. C.; Souza Filho, A. G.; Garcia, F.; Lima, S. M.; da Cunha Andrade, L. H.; Arruda, G. J.; Grillo, R.; Caires, A. R. L.; Felipe Santiago, E. Assessing the fate of superparamagnetic iron oxide nanoparticles carrying usnic acid as chemical cargo on the soil microbial community. *ACS Nano* **2023**, 17 (8), 7417–7430.
- (78) Yin, K.; Wang, Y.; Zhao, H. J.; Wang, D. X.; Guo, M. H.; Mu, M. Y.; Liu, Y. C.; Nie, X. P.; Li, B. Y.; Li, J. Y.; Xing, M. W. A comparative review of microplastics and nanoplastics: Toxicity hazards on digestive, reproductive and nervous system. *Sci. Total Environ.* **2021**, 774, No. 145758.
- (79) He, D. F.; Zhang, X. T.; Hu, J. N. Methods for separating microplastics from complex solid matrices: Comparative analysis. *J Hazardous Mater* **2021**, 409, No. 124640.
- (80) Hu, T.; Chen, J. A review on adsorption and transport of microplastics in soil and the effect of ageing on environmental behavior of pollutants. *Rock Mine Anal* **2022**, 41 (3), 353–363.
- (81) Tang, Y.; Zhang, S. H.; Su, Y. L.; Wu, D.; Zhao, Y. P.; Xie, B. Removal of microplastics from aqueous solutions by magnetic carbon nanotubes. *Chem Eng J* **2021**, 406, No. 126804.
- (82) Freiberg, Y.; Fine, P.; Borisover, M.; Levkovitch, I.; Baram, S. Biosolids increase phosphate adsorption of semi-arid Mediterranean soils. *J Environ Manage* **2022**, 305, No. 114361.
- (83) Griffiths, B. S.; Ritz, K.; Ebbelwhite, N.; Paterson, E.; Killham, K. Ryegrass rhizosphere microbial community structure under elevated carbon dioxide concentrations, with observations on wheat rhizosphere. *Soil Biol Biochem* **1998**, 30 (3), 315–321.
- (84) Sharma, D. K.; Andersen, S. B.; Ottosen, C. O.; Rosenqvist, E. Wheat cultivars selected for high Fv/Fm under heat stress maintain high photosynthesis, total chlorophyll, stomatal conductance, transpiration and dry matter. *Physiol Plant* **2015**, 153 (2), 284–298.

- (85) Li, Y.; Zhang, S.; Jiang, W.; Liu, D. Cadmium accumulation, activities of antioxidant enzymes, and malondialdehyde (MDA) content in *Pistia stratiotes* L. *Environ Sci Pollut Res Int* **2013**, *20* (2), 1117–23.
- (86) Ruiz-Perez, C. A.; Restrepo, S.; Zambrano, M. M. Microbial and functional diversity within the phyllosphere of espeletia species in an andean high-mountain ecosystem. *Appl Environ Microb* **2016**, *82* (6), 1807–1817.
- (87) Caporaso, J. G.; Lauber, C. L.; Walters, W. A.; Berg-Lyons, D.; Lozupone, C. A.; Turnbaugh, P. J.; Fierer, N.; Knight, R. Global patterns of 16S rRNA diversity at a depth of millions of sequences per sample. *P Natl Acad Sci USA* **2011**, *108*, 4516–4522.
- (88) Liu, C.; Cui, Y. M.; Li, X. Z.; Yao, M. J. microeco: an R package for data mining in microbial community ecology. *FEMS Microbiol Ecol* **2021**, *97* (2), 255.
- (89) Barberan, A.; Bates, S. T.; Casamayor, E. O.; Fierer, N. Using network analysis to explore co-occurrence patterns in soil microbial communities. *ISME J* **2012**, *6* (2), 343–351.